Document downloaded from:

http://hdl.handle.net/10251/124685

This paper must be cited as:

Lázaro, M. (2018). Eigensolutions of nonviscously damped systems based on the fixed-point iteration. Journal of Sound and Vibration. 418:100-121.
https://doi.org/10.1016/j.jsv.2017.12.025

The final publication is available at

https://doi.org/10.1016/j.jsv.2017.12.025

Copyright Elsevier

Additional Information

Eigensolutions of nonviscously damped systems based on the fixed-point iteration

M. Lázaro[a,*]

[a] *Department of Continuum Mechanics and Theory of Structures*
Universitat Politècnica de València 46022 Valencia, Spain

Abstract

In this paper, nonviscous, nonproportional, symmetric vibrating structures are considered. Nonviscously damped systems present dissipative forces depending on the time history of the response via kernel hereditary functions. Solutions of the free motion equation leads to a nonlinear eigenvalue problem involving mass, stiffness and damping matrices, this latter as dependent on frequency. Viscous damping can be considered as a particular case, involving damping forces as function of the instantaneous velocity of the degrees of freedom. In this work, a new numerical procedure to compute eigensolutions is proposed. The method is based on the construction of certain recursive functions which, under a iterative scheme, allow to reach eigenvalues and eigenvectors simultaneously and avoiding computation of eigensensitivities. Eigenvalues can be read then as fixed–points of those functions. A deep analysis of the convergence is carried out, focusing specially on relating the convergence conditions and error–decay rate to the damping model features, such as the nonproportionality and the viscoelasticity. The method is validated using two 6 degrees of freedom numerical examples involving both nonviscous and viscous damping and a continuous system with a local nonviscous damper. The convergence and the sequences behavior are in agreement with the results foreseen by the theory.

Keywords: fixed-point iteration, recursive functions, eigenvalues and eigenvectors, nonproportional damping, nonviscous damping, viscous damping

1. Introduction

Dynamical vibrating systems under viscous and nonviscous damping are considered. Nonviscous or viscoelastic materials have been widely used for vibrations control in many applications of mechanical, aerospace, automotive and civil engineering. Nonviscous damping models assume that dissipative forces are depending on the time history of the response velocity via hereditary kernel functions. This fact is represented in the motion equations by convolution integrals affecting to the velocities of the degrees–of–freedom (dof) over certain kernel functions. In general, the dof response, denoted by $\mathbf{u}(t) \in \mathbb{R}^N$, is governed by the following system of linear integro-differential equations

$$\mathbf{M}\ddot{\mathbf{u}} + \int_{-\infty}^{t} \boldsymbol{\mathcal{G}}(t-\tau)\,\dot{\mathbf{u}}\;\mathrm{d}\tau + \mathbf{K}\mathbf{u} = \mathfrak{f}(t) \tag{1}$$

where $\mathbf{M}$, $\mathbf{K} \in \mathbb{R}^{N\times N}$ are the mass and stiffness matrices assembled using the finite element method. We assume $\mathbf{M}$ to be positive definite and $\mathbf{K}$ positive semidefinite; $\boldsymbol{\mathcal{G}}(t) \in \mathbb{R}^{N\times N}$ is the nonviscous damping matrix in the time domain, assumed symmetric, which must satisfy the necessary conditions given by Golla and Hughes [1] to induce a strictly dissipative behavior. The viscous damping can be considered as a

*Corresponding author. Tel +34 963877000 (Ext. 76732). Fax +34 963877189
Email address: `malana@mes.upv.es` (M. Lázaro)

particular case with $\boldsymbol{\mathcal{G}}(t) \equiv \mathbf{C}\,\delta(t)$, where $\mathbf{C}$ is the viscous damping matrix and $\delta(t)$ the Dirac's delta function. The time–domain system of motion equations are then reduced to the well known expressions

$$\mathbf{M}\ddot{\mathbf{u}} + \mathbf{C}\dot{\mathbf{u}} + \mathbf{K}\mathbf{u} = \mathfrak{f}(t) \tag{2}$$

Let us consider the free–motion equation associated to Eq. (1), that is $\mathfrak{f}(t) \equiv \mathbf{0}$. Now, checking exponential solutions of the form $\mathbf{u}(t) = \boldsymbol{u}\,\mathrm{e}^{st}$, the nonlinear eigenvalue problem associated to viscoelastic vibrating structures is obtained

$$\left[s^2\mathbf{M} + s\mathbf{G}(s) + \mathbf{K}\right]\boldsymbol{u} \equiv \mathbf{D}(s)\,\boldsymbol{u} = \mathbf{0} \tag{3}$$

where $\mathbf{G}(s) = \mathcal{L}\{\boldsymbol{\mathcal{G}}(t)\} \in \mathbb{C}^{N\times N}$ is the damping matrix in the Laplace domain and $\mathbf{D}(s)$ is the dynamical stiffness matrix or transcendental matrix.

The time-domain response governed by Eqs. (1) and (2) is closely related to the eigensolutions of the associated nonlinear eigenvalue problem obtained in Eq. (3). For this type of dissipative models, Adhikari [2] derived modal relationships and closed form expressions for the transfer function in the frequency domain. Due to the nonlinearity, induced by a frequency-dependent damping matrix, the search eigensolutions is in general much more expensive from a computational point of view than that of classical viscous damping [3]. Hereditary damping models based on exponential kernels [4] and those based on the fractional derivatives [5, 6] are the most popular ones for engineering applications, although other several models can be found in the bibliography (for a survey of them see the references [7, 8]).

The problem of finding efficient numerical solutions is under permanent research due to the nonlinearity associated to Eq. (3). Mathematically, the problem is somehow closed for those damping models based on hereditary exponential kernels. These systems admit the introduction of certain auxiliary variables allowing to transform the N–sized nonlinear eigenvalue problem into an enlarged linear eigenvalue problem [9, 10, 11]. Otherwise, the introduction of these new internal variables increases the number of degrees of freedom and makes the method computationally expensive and in addition the physical insight is lost. To overcome the computational issue, numerical solutions based on the expansion of the transcendental matrix around an initial guess, results in locally quadratic convergence [12, 13, 14, 15], although the effectiveness depends on the chosen starting point. Asymptotic approaches using perturbation techniques of the damping matrix were carried out by Daya and Potier–Ferry [16] and by Duigou et al. [17]. Proportional or lightly nonproportional damped systems accept modal decoupling, reducing a N–sized matrix problem to a N decoupled modal algebraic equations. To solve them, Adhikari and Pascual [18, 19] proposed iterative approaches based on Taylor series expansion of the hereditary function in the frequency domain. We can also find methods which use the eigenvalue and eigenvector derivatives. For instance, in the references [20, 21, 22], some iterative procedures based on eigensensitivities are developed. Non–iterative approaches, deriving closed–form expressions of the eigenvalues, are proposed in references [23, 24]. Adhikari [25] proposed a recursive scheme valid for lightly nonproportional viscous damped systems which admitted eigenvector computation feedback.

In this paper, an efficient iterative method to obtain eigenvalues and eigenvectors of nonproportional nonviscous symmetric systems is proposed. Our approach is based on the construction of certain complex–valued functions, which possess the eigenvalues as fixed–points. An iterative scheme based on the recursive evaluation of these functions presents great benefits in the implementation due to its simplicity. Moreover, we can take advantage of the consolidated fixed–point theory to derive the conditions for convergence. This work is the continuation of a previous paper published by Lázaro et al. [8] where the procedure was developed for solving the decoupled single modal equations. Now, with this new procedure we overcome the problem of nonproportional systems obtaining simultaneously as well the complex eigenvectors in each iteration. Furthermore, since the derivative of the recursive function is closely related to the convergence properties of the method, we derive a closed form of that, obtaining interesting relationships between the convergence velocity and the damping model, that is, its nonproportionality and nonviscosity. The theoretical developments are validated through three numerical examples using both damping models (nonviscous and viscous). The numerical results show the scope of the method, proving that it is valid even for highly damped systems. In addition, a simple procedure to increase so predicted linear rate of convergence up to quadratic is proposed, specially for this type of recursive sequences.

2. Eigensolutions of nonviscous, nonproportional systems

In general, the eigensolutions of the nonlinear eigenproblem presented in Eq. (3) are formed by $2N + p$ eigenvalues and their associated eigenvectors [2] distributed as

$$\begin{aligned} &\{\lambda_1, \ldots, \lambda_N, \lambda_1^*, \ldots, \lambda_N^*\} \quad \cup \quad \{\lambda_{N+1}, \ldots, \lambda_{N+p}\} \\ &\{\mathbf{u}_1, \ldots, \mathbf{u}_N, \mathbf{u}_1^*, \ldots, \mathbf{u}_N^*\} \quad \cup \quad \{\mathbf{u}_{N+1}, , \ldots, \mathbf{u}_{N+p}\} \end{aligned} \tag{4}$$

The eigenvalues denoted by $\lambda_j, \ \lambda_j^* \in \mathbb{C}$ are complex conjugate pairs and they are responsible of the oscillatory nature to the time response. Their eigenvectors $\mathbf{u}_j, \ \mathbf{u}_j^* \in \mathbb{C}^N$ also form a set of N conjugate complex pairs. The eigenvalues denoted by λ_j, for $N + 1 \leq j \leq N + p$ are negative real numbers corresponding with the nonviscous modes and they are a consequence of the mathematical form of the hereditary functions within $\boldsymbol{\mathcal{G}}(t)$. They are associated to damping models based on exponential kernels [26, 27] and they are presented in a number directly related to the range of the limit viscous damping matrices [28, 3]. Lázaro [29] reduced the problem of finding these real eigenvalues to solve a finite set of linear eigenvalue problems. Their effect on the response can generally be neglected since they are associated with overdamped real modes and therefore their effect decay rapidly in time domain. We will focus on those modes $2N$ with oscillatory nature for which the modal relationships can be written as

$$\begin{aligned} \left[\lambda_j^2\mathbf{M} + \lambda_j\mathbf{G}(\lambda_j) + \mathbf{K}\right]\mathbf{u}_j \quad &\equiv \quad \mathbf{D}(\lambda_j)\mathbf{u}_j = \mathbf{0} \ , \ 1 \leq j \leq N \\ \left[\lambda_j^{*2}\mathbf{M} + \lambda_j^*\mathbf{G}(\lambda_j^*) + \mathbf{K}\right]\mathbf{u}_j^* \quad &\equiv \quad \mathbf{D}(\lambda_j^*)\mathbf{u}_j^* = \mathbf{0} \ , \ 1 \leq j \leq N \end{aligned} \tag{5}$$

In this paper, the eigensolutions of the undamped problem play an important role since they shape the construction of the eigenvectors sequence, as will be seen later. Imposing $\mathbf{G}(s) \equiv \mathbf{0}$ in Eq. (3), we define the undamped stiffness matrix as $\mathbf{D}_0(s) = s^2\mathbf{M} + \mathbf{K}$. The natural frequencies $\omega_j \in \mathbb{R}$ and the undamped eigenvectors, respectively denoted by $\boldsymbol{\phi}_j \in \mathbb{R}^N$, are related through

$$\mathbf{K}\boldsymbol{\phi}_j = \omega_j^2\mathbf{M}\boldsymbol{\phi}_j \ , \ 1 \leq j \leq N \tag{6}$$

Assuming that there are not repeated frequencies, we can mass–normalize the eigenvectors using the biorthogonality relations are

$$\boldsymbol{\phi}_j^{\intercal}\mathbf{M}\boldsymbol{\phi}_k = \delta_{jk} \ , \quad \boldsymbol{\phi}_j^{\intercal}\mathbf{K}\boldsymbol{\phi}_k = \omega_j^2\,\delta_{jk} \ , \quad \boldsymbol{\phi}_j^{\intercal}\mathbf{G}(s)\boldsymbol{\phi}_k = \Gamma_{jk}(s) \tag{7}$$

where δ_{jk} is the Kronecker delta. In general, the damping matrix does not become diagonal in the modal space of the undamped problem. Mathematically, the eigenvectors $\boldsymbol{\phi}_j$ can be arranged as the columns of the following square matrix (modal matrix)

$$\boldsymbol{\Phi} = [\boldsymbol{\phi}_1, \ldots, \boldsymbol{\phi}_N] \in \mathbb{R}^{N\times N} \tag{8}$$

Then, from Eqs. (7), we have

$$\boldsymbol{\Phi}^{\intercal}\,\mathbf{M}\,\boldsymbol{\Phi} = \mathbf{I}_N \ , \quad \boldsymbol{\Phi}^{\intercal}\,\mathbf{K}\,\boldsymbol{\Phi} = \boldsymbol{\Omega}^2 \ , \quad \boldsymbol{\Phi}^{\intercal}\,\mathbf{G}(s)\,\boldsymbol{\Phi} = \boldsymbol{\Gamma}(s) \tag{9}$$

where $\mathbf{I}_N \in \mathbb{R}^{N\times N}$ denotes the identity matrix and $\boldsymbol{\Omega} = \mathrm{diag}\,[\omega_1, \ldots, \omega_N]$ is a diagonal matrix with the natural frequencies located in the main diagonal. $\boldsymbol{\Gamma}(s)$ denotes the modal damping matrix. Those systems in which $\boldsymbol{\Gamma}(s)$ becomes exactly diagonal are said to be classically or proportionally damped. Caughey and O'Kelly [30] studied the necessary and sufficient conditions for proportional damping in symmetric viscous systems. And furthermore, those conditions for exact proportional damping in nonviscously damped structures were provided by Adhikari [31].

Adhikari [32, 2] proved that complex eigenvectors are closely related to the nondiagonal elements of the modal damping matrix and proposed a method to obtain them using Neuman expansion series. Let us revisit the Adhikari's algorithm to calculate the jth eigenvector since part of the current proposed method is constructed from it. Let us assume that the jth complex eigenvalue λ_j of Eq. (3) is known. In order to find $\mathbf{u}_j$ we can proceed expanding this latter as linear combination of the undamped eigenvectors' base, that is

$$\mathbf{u}_j = \sum_{k=1}^{N} a_{jk} \boldsymbol{\phi}_k \tag{10}$$

reducing the problem to calculate corresponding unknown coefficients $a_k^{(j)}$. Without loss of generality we can assume that $a_{jj} = 1$ so that the unknown coefficients can be arranged in the following column vector of size $(N-1)$

$$\mathbf{a}_j = \{a_{j1}, \ldots, a_{j\,j-1}, a_{j\,j+1}, \ldots, a_{jN}\}^\intercal \in \mathbb{C}^{N-1} \tag{11}$$

Adhikari [2] obtained the above vector as solution of the linear system of size $(N-1)\times(N-1)$

$$[\mathbf{P}_j - \mathbf{Q}_j]\, \mathbf{a}_j = \mathbf{g}_j \tag{12}$$

where

$$\mathbf{P}_j = -\frac{1}{\lambda_j} \operatorname{diag}\left[d_1(\lambda_j), \ldots, d_{j-1}(\lambda_j), d_{j+1}(\lambda_j), \ldots, d_N(\lambda_j)\right] \in \mathbb{C}^{(N-1)\times(N-1)} \tag{13}$$

$$\mathbf{g}_j = \{\Gamma_{1j}(\lambda_j), \ldots, \Gamma_{j-1\,j}(\lambda_j), \Gamma_{j+1\,j}(\lambda_j), \ldots, \Gamma_{Nj}(\lambda_j)\}^\intercal \in \mathbb{C}^{N-1} \tag{14}$$

and $d_k(\lambda_j) = \lambda_j^2 + \lambda_j \Gamma_{kk}(\lambda_j) + \omega_k^2$. $\mathbf{Q}_j \in \mathbb{C}^{(N-1)\times(N-1)}$ is a traceless matrix constructed from $\boldsymbol{\Gamma}(\lambda_j)$ after deleting the jth row and column and making null the entrees of the main diagonal, i.e.

$$\mathbf{Q}_j = \begin{bmatrix} 0 & \Gamma_{12}(\lambda_j) & \cdots & \Gamma_{1,j-1}(\lambda_j) & (j\text{th del.}) & \Gamma_{1,j+1}(\lambda_j) & \cdots & \Gamma_{1N}(\lambda_j) \\ \Gamma_{21}(\lambda_j) & 0 & \cdots & \Gamma_{2,j-1}(\lambda_j) & (j\text{th del.}) & \Gamma_{2,j+1}(\lambda_j) & \cdots & \Gamma_{2N}(\lambda_j) \\ \vdots & \vdots & \ddots & \vdots & \vdots & \vdots & \cdots & \vdots \\ \Gamma_{j-1,1}(\lambda_j) & \Gamma_{j-1,2}(\lambda_j) & \cdots & 0 & (j\text{th del.}) & \Gamma_{j-1,j+1}(\lambda_j) & \cdots & \Gamma_{j-1,N}(\lambda_j) \\ (j\text{th del.}) & (j\text{th del.}) & \cdots & (j\text{th del.}) & (j\text{th del.}) & (j\text{th del.}) & \cdots & (j\text{th del.}) \\ \Gamma_{j+1,1}(\lambda_j) & \Gamma_{j+1,2}(\lambda_j) & \cdots & \Gamma_{j+1,j-1}(\lambda_j) & (j\text{th del.}) & 0 & \cdots & \Gamma_{j+1,N}(\lambda_j) \\ \vdots & \vdots & \vdots & \vdots & \vdots & \vdots & \ddots & \vdots \\ \Gamma_{N1}(\lambda_j) & \Gamma_{N2}(\lambda_j) & \cdots & \Gamma_{N,j-1}(\lambda_j) & (j\text{th del.}) & \Gamma_{N,j+1}(\lambda_j) & \cdots & 0 \end{bmatrix} \tag{15}$$

Denoting by $\mathbf{R}_j = \mathbf{P}_j^{-1}\mathbf{Q}_j$ and $\mathbf{a}_{j0} = \mathbf{P}_j^{-1}\mathbf{g}_j$, the unknown vector $\mathbf{a}_j$ can be obtained from the Neuman expansion

$$\mathbf{a}_j = \mathbf{a}_{j0} + \mathbf{a}_{j1} + \mathbf{a}_{j2} + \cdots \tag{16}$$

where $\mathbf{a}_{jn} = \mathbf{R}_j\, \mathbf{a}_{j,n-1} = \mathbf{R}_j^n\, \mathbf{a}_{j0}$, provided that $\|\mathbf{R}_j\| < 1$ for some induced matrix norm. According to the reference [2], this condition holds if $\boldsymbol{\Gamma}(\lambda_j)$ is a diagonally dominant matrix. The previous condition based on the matrix norm is necessary and sufficient. Adhikari [2] proved that a sufficient condition to guarantee the expansion (16) is the diagonal dominance of $\boldsymbol{\Gamma}(\lambda_j)$, that is

$$\sum_{\substack{l=1 \\ l\neq j\neq k}}^{N} |\Gamma_{kl}(\lambda_j)| < |\Gamma_{kk}(\lambda_j)| \ , \qquad \forall\, k \neq j \tag{17}$$

In the most general case, we can write the complex eigenvector as the closed form

$$\mathbf{u}_j = \boldsymbol{\phi}_j + \boldsymbol{\Phi}_j\, \mathbf{a}_j = \boldsymbol{\phi}_j + \boldsymbol{\Phi}_j\, \left(\mathbf{P}_j - \mathbf{Q}_j\right)^{-1} \mathbf{g}_j \tag{18}$$

where

$$\boldsymbol{\Phi}_j = \left[\boldsymbol{\phi}_1\ \ldots\ \boldsymbol{\phi}_{j-1}\, (j\text{th del.})\, \boldsymbol{\phi}_{j+1}, \ldots\, \boldsymbol{\phi}_N\right] \in \mathbb{R}^{N\times(N-1)} \tag{19}$$

is the modal matrix after deleting the jth mode. Eq. (18) is function on the modal damping coefficients, the natural frequencies and the complex eigenvalues. Except these latter, the rest of information is known before solving the nonlinear eigenvalue problem. We will take advance on this fact in order to construct our recursive functions in the following section

3. Fixed–point recursive scheme

This section is aimed at deriving the fundamentals of the proposed method. The final objective is to build $2N$ complex–valued functions, which will be denoted henceforth by $X_j(s), Y_j(s), 1 \leq j \leq N$, so that the iterative scheme based on the recursion of these two functions converges to the conjugate complex pair λ_j, λ_j^*, respectively. With recursion we mean the successive evaluation of the functions with values obtained in previous iteration, that is

$$x_j^{(n+1)} = X_j\left(x_j^{(n)}\right) \ , \quad y_j^{(n+1)} = Y_j\left(y_j^{(n)}\right) \ , \quad n = 0, 1, 2, \ldots \tag{20}$$

where the index n denote the iteration. Under these conditions it is said that λ_j and λ_j^* are fixed points of the functions $X_j(s)$ and $Y_j(s)$, respectively. In mathematical form,

$$\lambda_j = X_j(\lambda_j) \ , \quad \lambda_j^* = Y_j(\lambda_j^*) \tag{21}$$

In the process of defining $X_j(s)$ and $Y_j(s)$, we distinguish between proportional and nonproportional damping. Although the former can be consider as a particular case of this latter, we proceed from the simplest to the most complex problem for a sake of clarity in our exposition.

3.1. Proportional damping

This case has already been addressed by Lázaro et al. [8] and the most interesting results will be summarized at this point. We consider necessary to present this background in order to a better comprehension of our approach since the structure of the recursive function presents certain similarities with that for nonproportionally damped systems, which will be developed later. Assuming then that the damping matrix $\mathbf{G}(s)$ verifies the conditions given Adhikari [31] for proportional damping, then the system of N dofs is transformed into N decoupled single dof systems under the base change of the modal damping matrix of undamped problem. The damping matrix becomes diagonal, so that

$$\boldsymbol{\phi}_j^{\mathsf{T}} \mathbf{G}(s) \boldsymbol{\phi}_k = \Gamma_{jk}(s) = \Gamma_{jj}(s)\, \delta_{jk} \ , \quad \forall\, s \in \mathbb{C}$$

Hence, the pair of conjugate complex eigenvalues λ_j, λ_j^* are the roots of the modal equation

$$\mathcal{D}_j(s) = \boldsymbol{\phi}_j^{\mathsf{T}}\, \mathbf{D}(s)\, \boldsymbol{\phi}_j = s^2 + s\Gamma_{jj}(s) + \omega_j^2 = 0 \tag{22}$$

Let us introduce the dimensionless damping function

$$\mathcal{J}_j(s) = \frac{\boldsymbol{\phi}_j^{\mathsf{T}} \mathbf{G}(s) \boldsymbol{\phi}_j}{2\omega_j} = \frac{\Gamma_{jj}(s)}{2\omega_j} \tag{23}$$

After some straight operations we can express $\mathcal{D}_j(s)$ as a product of functions. Indeed,

$$\begin{aligned} \mathcal{D}_j(s) &= s^2 + 2s\mathcal{J}_j(s)\,\omega_j + \omega_j^2 = [s + \omega_j \mathcal{J}_j(s)]^2 + \omega_j\left[1 - \mathcal{J}_j^2(s)\right] \\ &= [s + \omega_j \mathcal{J}_j(s)]^2 - \left[\mathrm{i}\,\omega_j \sqrt{1 - \mathcal{J}_j^2(s)}\right]^2 \equiv [s - X_j(s)]\,[s - Y_j(s)] \end{aligned} \tag{24}$$

where

$$X_j(s) = \omega_j \left[-\mathcal{J}_j(s) + \mathrm{i}\sqrt{1 - \mathcal{J}_j^2(s)}\right] \quad , \quad Y_j(s) = \omega_j \left[-\mathcal{J}_j(s) - \mathrm{i}\sqrt{1 - \mathcal{J}_j^2(s)}\right] \tag{25}$$

In the above expressions $\mathrm{i} = \sqrt{-1}$ is the imaginary unity and $\sqrt{\bullet}$ is the main square root of a complex number. We assume that $\Gamma_{jj}(s)$ verifies the necessary conditions given by [1] to induce a strictly dissipative motion. Additionally, we will assume that $\Gamma_{jj}(s)$ satisfies the following two mathematical hypothesis

H1 $\Gamma_{jj}(s)$ is analytic in $\mathbb{C}\setminus\mathbb{R}$ (complex plane excluded the real numbers)

H2 $\Gamma_{jj}(s)$ transforms nonreal complex numbers into nonreal complex numbers, i.e. if $\Im\{s\}\neq 0$ then $\Im\{J_j(s)\}\neq 0$

Under these hypothesis Lázaro et al. [8] proved that taking two symmetrical initial points $x_j^{(0)}$ and $y_j^{(0)} = x_j^{(0)*}$ we can build two recursive sequences as

$$x_j^{(n+1)} = X_j\left(x_j^{(n)}\right) \quad , \quad y_j^{(n+1)} = Y_j\left(y_j^{(n)}\right) \quad , \quad n = 0,1,2,\ldots \tag{26}$$

and we can ensure that

P1. $\lambda_j = \lim_{n\to\infty} x_j^{(n)}$, $\lambda_j^* = \lim_{n\to\infty} y_j^{(n)}$

P2. $\lambda_j = X_j(\lambda_j)$ if and only if $\lambda_j^* = Y_j(\lambda_j^*)$

P3. $\Im\{X_j(s)\} > 0$ and $\Im\{Y_j(s)\} < 0$, $\forall s\in\mathbb{C}\setminus\mathbb{R}$

Note that according to the third conclusion, the sequence $\{x_j^{(n)}\}_{n=1}^{\infty}$ is always contained inside the upper half complex plane, while $\{y_j^{(n)}\}_{n=1}^{\infty}$ is within the lower one. Moreover, in the complex plane both paths draw symmetric sequences respect to the real axis. In reference to real eigenvalues, it is not possible to know a priori whether they are fixed points of $X_j(s)$ or $Y_j(s)$. Numerical examples of [8] shown up global convergence, so that solutions of the sequences' limits were always found, even for highly damped systems.

3.2. Nonproportional damping

Eigenvalues of damped systems under light nonproportionality can be solved using the decoupled scheme describe above. Then, complex eigenvectors can be estimated using one or two terms in the Neuman expansion of Adhikari (see Eq. (16)). This procedure works accurately for a great number of structures since the light nonproportionality is commonly assumed in structural dynamics. However, in order to address any level of nonproportionality our goal is to include the complex eigenvectors also in the iterative process but keeping the same properties for the recursive functions, so that certain properties already proved in [8] can be extrapolated here.

In a first step, we will define N vector functions $\boldsymbol{\mathcal{U}}_j(s):\mathbb{C}\to\mathbb{C}^N,\ 1\leq j\leq N$ depending on the Laplace parameter $s\in\mathbb{C}$. These functions will be designed so that the returned vector at $s=\lambda_j$ is precisely the complex mode, i.e. $\mathbf{u}_j = \boldsymbol{\mathcal{U}}_j(\lambda_j)$. From the previously shown expressions to obtain $\mathbf{u}_j$, we note that matrices $\mathbf{P}_j$, $\mathbf{Q}_j$ and $\mathbf{g}_j$ of Eqs. (13), (14) and (15), depend directly on λ_j. This observation leads us to define $\boldsymbol{\mathcal{U}}_j(s)$ as

$$\boldsymbol{\mathcal{U}}_j(s) = \boldsymbol{\phi}_j + \sum_{\substack{k=1\\k\neq j}}^{N}\alpha_{jk}(s)\,\boldsymbol{\phi}_k \tag{27}$$

where the $N-1$ functions $\alpha_{jk}(s)$ can also be arranged in a vector function of s, with the same structure as Eq. (11).

$$\boldsymbol{\alpha}_j(s) = \{\alpha_{j1}(s),\ldots,\alpha_{j\,j-1}(s),\alpha_{j\,j+1}(s),\ldots,\alpha_{jN}(s)\}^{\intercal}\in\mathbb{C}^{N-1} \tag{28}$$

For each $s\in\mathbb{C}$, $\boldsymbol{\alpha}_j(s)$ is calculated from the solution of the s-dependent linear system

$$\left[\boldsymbol{\mathcal{P}}_j(s) - \boldsymbol{\mathcal{Q}}_j(s)\right]\boldsymbol{\alpha}_j(s) = \boldsymbol{g}_j(s) \tag{29}$$

where now

$$\begin{aligned}
\boldsymbol{\mathcal{P}}_j(s) &= -\frac{1}{s}\,\mathrm{diag}\left[d_1(s),\ldots,d_{j-1}(s),d_{j+1}(s),\ldots,d_N(s)\right]\in\mathbb{C}^{(N-1)\times(N-1)} && (30)\\
\boldsymbol{g}_j(s) &= \{\Gamma_{1j}(s),\ldots,\Gamma_{j-1\,j}(s),\Gamma_{j+1\,j}(s),\ldots,\Gamma_{Nj}(s)\}^{\intercal}\in\mathbb{C}^{N-1} && (31)\\
d_k(s) &= s^2 + s\Gamma_{kk}(s) + \omega_k^2
\end{aligned}$$

and $\boldsymbol{\mathcal{Q}}_j(s) \in \mathbb{C}^{(N-1)\times(N-1)}$ is obtained from $\boldsymbol{\Gamma}(s)$ after making the main diagonal null and deleting the jth row and jth column, namely

$$\boldsymbol{\mathcal{Q}}_j(s) = \begin{bmatrix} 0 & \Gamma_{12}(s) & \cdots & \Gamma_{1,j-1}(s) & (j\text{th del.}) & \Gamma_{1,j+1}(s) & \cdots & \Gamma_{1N}(s) \\ \Gamma_{21}(s) & 0 & \cdots & \Gamma_{2,j-1}(s) & (j\text{th del.}) & \Gamma_{2,j+1}(s) & \cdots & \Gamma_{2N}(s) \\ \vdots & \vdots & \ddots & \vdots & \vdots & \vdots & \cdots & \vdots \\ \Gamma_{j-1,1}(s) & \Gamma_{j-1,2}(s) & \cdots & 0 & (j\text{th del.}) & \Gamma_{j-1,j+1}(s) & \cdots & \Gamma_{j-1,N}(s) \\ (j\text{th del.}) & (j\text{th del.}) & \cdots & (j\text{th del.}) & (j\text{th del.}) & (j\text{th del.}) & \cdots & (j\text{th del.}) \\ \Gamma_{j+1,1}(s) & \Gamma_{j+1,2}(s) & \cdots & \Gamma_{j+1,j-1}(s) & (j\text{th del.}) & 0 & \cdots & \Gamma_{j+1,N}(s) \\ \vdots & \vdots & \vdots & \vdots & \vdots & \vdots & \ddots & \vdots \\ \Gamma_{N1}(s) & \Gamma_{N2}(s) & \cdots & \Gamma_{N,j-1}(s) & (j\text{th del.}) & \Gamma_{N,j+1}(s) & \cdots & 0 \end{bmatrix} \tag{32}$$

The so-defined function verifies that $\boldsymbol{\mathcal{U}}_j(\lambda_j) = \mathbf{u}_j$; furthermore, since $\boldsymbol{\mathcal{U}}_j(s)$ is continuous at $\lambda_j \in \mathbb{C}$, any complex sequence convergent to the jth complex eigenvalue, $\{x^{(n)}\} \to \lambda_j$, results in a vectors sequence convergent to the jth complex eigenvector, i.e. $\{\boldsymbol{u}^{(n)} = \boldsymbol{\mathcal{U}}_j(x^{(n)})\} \to \mathbf{u}_j$. Like $\mathbf{u}_j$ in Eq. (18), the function $\boldsymbol{\mathcal{U}}_j(s)$ also admits a closed expression, function on s

$$\boldsymbol{\mathcal{U}}_j(s) = \boldsymbol{\phi}_j + \boldsymbol{\Phi}_j\, \boldsymbol{\alpha}_j(s) = \boldsymbol{\phi}_j + \boldsymbol{\Phi}_j\, \left[\boldsymbol{\mathcal{P}}_j(s) - \boldsymbol{\mathcal{Q}}_j(s)\right]^{-1} \boldsymbol{g}_j(s) \tag{33}$$

although the most efficient way to find $\boldsymbol{\alpha}_j(s)$ is solving numerically the linear system (29) for each s, rather than computing the inverse matrix.

As second step, we will derive now the recursive functions for the nonproportional case with help of the new defined functions $\boldsymbol{\mathcal{U}}_j(s)$. Let us define the modal equation associated to the jth mode as

$$\mathcal{D}_j(s) = \frac{\boldsymbol{\mathcal{U}}_j^{\mathsf{H}}(s)\, \mathbf{D}(s) \boldsymbol{\mathcal{U}}_j(s)}{\boldsymbol{\mathcal{U}}_j^{\mathsf{H}}(s)\, \mathbf{M} \boldsymbol{\mathcal{U}}_j(s)} \tag{34}$$

where $\boldsymbol{u}^{\mathsf{H}} = (\boldsymbol{u}^*)^{\mathsf{T}}$ represents the conjugate-transpose vector (Hermitian transpose). Since $\mathbf{M}$ is positive definite, $\boldsymbol{u}^{\mathsf{H}}\, \mathbf{M}\boldsymbol{u} > 0$, for any complex N-dimensional vector $\boldsymbol{u} \neq \mathbf{0}$ and therefore $\mathcal{D}_j(s)$ is well defined in Eq. (34). Note that we are using the same notation as that of proportional damping because this latter is in fact a particular case of the nonproportional systems. Indeed, $\boldsymbol{\mathcal{U}}_j(s) \equiv \boldsymbol{\phi}_j$ for proportional damping. Furthermore, the use of the same notation helps us to compare the parallelism between both cases. Expanding the dynamical stiffness matrix and after some straight operations in Eq. (34) we obtain

$$\mathcal{D}_j(s) \quad = \quad s^2 + s\, \frac{\boldsymbol{\mathcal{U}}_j^{\mathsf{H}}(s)\, \mathbf{G}(s) \boldsymbol{\mathcal{U}}_j(s)}{\boldsymbol{\mathcal{U}}_j^{\mathsf{H}}(s)\, \mathbf{M} \boldsymbol{\mathcal{U}}_j(s)} + \frac{\boldsymbol{\mathcal{U}}_j^{\mathsf{H}}(s)\, \mathbf{K} \boldsymbol{\mathcal{U}}_j(s)}{\boldsymbol{\mathcal{U}}_j^{\mathsf{H}}(s)\, \mathbf{M} \boldsymbol{\mathcal{U}}_j(s)} \tag{35}$$

Let us introduce now the following functions $\mathcal{W}_j(s) : \mathbb{C} \to \mathbb{R}^+$ and $\mathcal{J}_j(s) : \mathbb{C} \to \mathbb{C}$ defined as

$$\mathcal{W}_j(s) = \sqrt{\frac{\boldsymbol{\mathcal{U}}_j^{\mathsf{H}}(s)\, \mathbf{K} \boldsymbol{\mathcal{U}}_j(s)}{\boldsymbol{\mathcal{U}}_j^{\mathsf{H}}(s)\, \mathbf{M} \boldsymbol{\mathcal{U}}_j(s)}} \quad , \quad \mathcal{J}_j(s) = \frac{\boldsymbol{\mathcal{U}}_j^{\mathsf{H}}(s)\, \mathbf{G}(s) \boldsymbol{\mathcal{U}}_j(s)}{2\, \mathcal{W}_j(s) \boldsymbol{\mathcal{U}}_j^{\mathsf{H}}(s)\, \mathbf{M} \boldsymbol{\mathcal{U}}_j(s)} \tag{36}$$

Since $\mathbf{K}$ and $\mathbf{M}$ are positive semidefinite and definite respectively, the inequalities $\boldsymbol{u}^{\mathsf{H}}\mathbf{K}\boldsymbol{u} \geq 0$ and $\boldsymbol{u}^{\mathsf{H}}\mathbf{M}\boldsymbol{u} > 0$ hold for any nonzero complex vector $\boldsymbol{u} \in \mathbb{C}^N$. Hence, $\mathcal{W}_j(s)$ is well defined and it is always a positive real number (except for solid–rigid modes, which are not considered in this problem). Moreover, $\mathcal{W}_j(s)$ has units of frequency and coincides with the natural frequency if the system becomes proportional. In addition, $\mathcal{J}_j(s)$ is a dimensionless representation of the damping function very similar to that presented in Eq. (23). Again that one is a particular case of that of Eq. (36) when the system is proportional. Under these assumptions

$\mathcal{D}_j(s)$ adopts a form quite similar to that of Eq. (24), so that the same manipulations can be carried out, obtaining

$$\begin{aligned}
\mathcal{D}_j(s) &= s^2 + 2s\mathcal{J}_j(s)\,\mathcal{W}_j(s) + \mathcal{W}_j^2(s) = [s + \mathcal{W}_j(s)\mathcal{J}_j(s)]^2 + \mathcal{W}_j(s)\left[1 - \mathcal{J}^2(s,\boldsymbol{u})\right] \\
&= [s + \mathcal{W}_j(s)\mathcal{J}_j(s)]^2 - \left[i\,\mathcal{W}_j(s)\sqrt{1-\mathcal{J}_j^2(s)}\right]^2 \equiv [s - X_j(s)]\,[s - Y_j(s)]
\end{aligned} \tag{37}$$

where

$$X_j(s) = \mathcal{W}_j(s)\,\left[-\mathcal{J}_j(s) + \mathrm{i}\sqrt{1-\mathcal{J}_j^2(s)}\right] \quad , \quad Y_j(s) = \mathcal{W}_j(s)\,\left[-\mathcal{J}_j(s) - \mathrm{i}\sqrt{1-\mathcal{J}_j^2(s)}\right] \tag{38}$$

The single-variable functions $X_j(s), Y_j(s)$ can be used within a fixed-point iterative scheme leading to the two following sequences of complex numbers

$$x_j^{(n+1)} = X_j\left(x_j^{(n)}\right) \quad , \quad y_j^{(n+1)} = Y_j\left(y_j^{(n)}\right) \quad , \quad n = 0, 1, 2, \ldots \tag{39}$$

Assuming that $\mathcal{J}_j(s)$ verifies the same hypothesis H1 and H2, imposed in the previous point, then we can ensure that both sequences are symmetric respect to the real axis provided that the two starting points are also conjugate–complex, or $y_j^{(0)} = x_j^{(0)^*}$. The vectors' sequences can be obtained applying $\boldsymbol{\mathcal{U}}_j(s)$ to $\{x_j^{(n)}\}$ and $\{y_j^{(n)}\}$ as

$$\boldsymbol{u}_j^{(n)} = \boldsymbol{\mathcal{U}}_j\left(x_j^{(n)}\right) \quad , \quad \boldsymbol{v}_j^{(n)} = \boldsymbol{\mathcal{U}}_j\left(y_j^{(n)}\right) \tag{40}$$

If $\{x_j^{(n)}\}$, $\{y_j^{(n)}\}$ are convergent, then the eigensolutions of the nonproportional system can be calculated as the limits

$$\lambda_j = \lim_{n\to\infty} x_j^{(n)} \quad , \quad \lambda_j^* = \lim_{n\to\infty} y_j^{(n)} \quad , \quad \mathbf{u}_j = \lim_{n\to\infty} \boldsymbol{u}_j^{(n)} \quad , \quad \mathbf{u}_j^* = \lim_{n\to\infty} \boldsymbol{v}_j^{(n)} \tag{41}$$

The highest computational effort in each iteration comes from solving the $(N-1)$–sized linear system (29). However, if the system can be considered lightly nonproportional, the computational cost in the calculation of $\boldsymbol{u}_j^{(n)}$ in each iteration can significantly be reduced just using the Neuman expansion series of Eq. (33). Indeed, denoting by

$$\boldsymbol{\mathcal{R}}_j(s) = \boldsymbol{\mathcal{P}}_j^{-1}(s)\,\boldsymbol{\mathcal{Q}}_j(s)$$

then we can approximate

$$\boldsymbol{\alpha}_j(s) = \boldsymbol{\alpha}_{j0}(s) + \boldsymbol{\alpha}_{j1}(s) + \boldsymbol{\alpha}_{j2}(s) + \cdots \tag{42}$$

where $\boldsymbol{\alpha}_{j,n}(s) = \boldsymbol{\mathcal{R}}_j(s)\,\boldsymbol{\alpha}_{j,n-1}(s) = \boldsymbol{\mathcal{R}}_j^n(s)\,\boldsymbol{\alpha}_{j0}(s)$, provided that $\|\boldsymbol{\mathcal{R}}_j(s)\| < 1$. Remember that $\boldsymbol{\mathcal{P}}_j(s)$ is a diagonal matrix, hence the computation of its inverse is straightforward. Under these assumptions, the second order approximation of $\boldsymbol{\mathcal{U}}_j(s)$ has the expression

$$\boldsymbol{\mathcal{U}}_j(s) = \boldsymbol{\phi}_j - s\sum_{\substack{k=1\\k\neq j}}^{N} \frac{\Gamma_{kj}(s)}{d_k(s)}\,\boldsymbol{\phi}_k + s^2 \sum_{\substack{k=1\\k\neq j}}^{N} \sum_{\substack{l=1\\l\neq j\neq k}}^{N} \frac{\Gamma_{kl}(s)\Gamma_{lj}(s)}{d_k(s)\,d_l(s)}\,\boldsymbol{\phi}_k \tag{43}$$

Note that if the sequences $\{x_j^{(n)}, \boldsymbol{u}^{(n)}\}$ converge under this approach, they do not reach the exact eigenpair $(\lambda_j, \mathbf{u}_j)$, but an approximation of them compatible with the hypothesis of light nonproportional damping. Otherwise, the computational effort of the sequences evaluation notably diminish.

3.3. Summary of algorithm

The proposed ideas presented in this section can be implemented as a simple algorithm. Assuming that the undamped solutions $\mathrm{i}\omega_j, \boldsymbol{\phi}_j$ $j = 1, \ldots, N$ are known, then the N complex eigenvalues (with positive real value) and their corresponding eigenmodes can be found using the recursive alghorithm shown in Table 1

Table 1: Algorithm of the proposed numerial method

for $j = 1, 2, \ldots, N$ **do**			**Equations**
Initialize $\epsilon = 100, \ n = 0$			
$x_j^{(0)} = \mathrm{i}\omega_j$			
while $\epsilon > \epsilon_{\mathbf{max}}$			
	$s = x_j^{(n)}$		
	Evaluate	$\boldsymbol{\mathcal{P}}_j(s), \boldsymbol{\mathcal{Q}}_j(s), \boldsymbol{g}_j(s)$	(30),(31),(32)
	Solve	$\left[\boldsymbol{\mathcal{P}}_j(s) - \boldsymbol{\mathcal{Q}}_j(s)\right] \boldsymbol{\alpha}_j(s) = \boldsymbol{g}_j(s)$	(29)
	Evaluate	$\boldsymbol{\mathcal{U}}_j(s) = \boldsymbol{\phi}_j + \boldsymbol{\Phi}_j \, \boldsymbol{\alpha}_j(s)$	(33)
	Evaluate	$\mathcal{W}_j(s), \mathcal{J}_j(s)$	(36)
	Evaluate	$x_j^{(n+1)} = X_j(s)$	(38)
	Evaluate	$\epsilon = \left\vert x_j^{(n+1)} - x_j^{(n)} \right\vert / \left\vert x_j^{(n)} \right\vert$	
	Update	$n = n + 1$	
end while			
$\lambda_j = x_j^{(n)}$			
Evaluate	$\boldsymbol{\mathcal{P}}_j(\lambda_j), \boldsymbol{\mathcal{Q}}_j(\lambda_j), \boldsymbol{g}_j(\lambda_j)$		(30),(31),(32)
Solve	$\left[\boldsymbol{\mathcal{P}}_j(s) - \boldsymbol{\mathcal{Q}}_j(\lambda_j)\right] \mathbf{a}_j = \boldsymbol{g}_j(\lambda_j)$		(29)
Evaluate	$\mathbf{u}_j = \boldsymbol{\phi}_j + \boldsymbol{\Phi}_j \, \mathbf{a}_j$		(33)
end for			

It can be noted that this method does not require partial evaluations of eigenmodes derivatives or sensitivities, something that notably simplifies the algorithm. The main computational effort is focused on computing the linear system needed to find $\boldsymbol{\alpha}_j(x_j^{(n)})$ in every iteration.

The new fixed–point scheme based on the recursion of $X_j(s)$ and $Y_j(s)$ in their general forms for nonproportional systems is the most important contribution of this paper. We consider that this development must be necessarily completed with an exhaustive analysis of the convergence. Lázaro et al. [8] studied the conditions for global and local convergence for proportional systems using for that some special results on fixed–point theory. From a numerical point of view, an interesting result obtained in that work is the close relationship between the level of viscoelasticity, that is the derivative $\Gamma'_{jj}(\lambda_j)$, and the velocity of convergence. In the next section, the analysis of convergence will show further results for nonproportional systems. In fact, we will demonstrate that not only the viscoelasticity but also the level of nonproportionality affects to the convergence velocity. Additionally, interesting conclusions respect to its application for viscous systems not seen in previous works will be derived

4. Analysis of convergence

Let us consider the general case of nonproportional systems, considering for that any symmetric damping matrix $\mathbf{G}(s)$. The fixed-point iteration of $X_j(s)$ and $Y_j(s)$ defined in Eq. (38) results in the sequences $\{x_j^{(n)}\}, \{y_j^{(n)}\}$ of Eq. (39). According to the general theory of self–mappings in Banach spaces [33], the local convergence of both sequences up to $\lambda_j, \ \lambda_j^*$ is directly related with the value of the s-derivatives of the recursive function evaluated at the eigenvalues, say $\left\vert X'_j(\lambda_j) \right\vert$ and $\left\vert Y'_j(\lambda_j^*) \right\vert$. Thus, three cases can be distinguished [33]

i) $\left\vert X'_j(\lambda_j) \right\vert < 1$. The sequence $\{x_j^{(n)}\}$ locally converges up to λ_j with linear velocity. In this case, the fixed point λ_j is said to be *attractive*. Furthermore, if in addition the equality $\left\vert X'_j(\lambda_j) \right\vert = 0$ holds, then the sequence locally converges with quadratic velocity.

ii) $\left\vert X'_j(\lambda_j) \right\vert = 1$. The local convergence is not guaranteed up to the fixed point. If convergence holds, it does under sub-linear velocity. Otherwise, the sequence enters into an infinite nonconvergent loop or diverges.

iii) $\left|X_j'(\lambda_j)\right| > 1$. The sequences $\{x_j^{(n)}\}$ do not converge to λ_j, even if initial guesses close to λ_j are chosen. In this case, the fixed point λ_j is said to be *repulsive*.

The same discussion can be made for $Y_j(s)$ and its associated sequence $\{y_j^{(n)}\}$. Therefore and without loss of generality, the developments will be only presented for $\{x_j^{(n)}\}$ and for $X_j(s)$ due to the proved parallelism between both functions, from properties P1, P2 and P3.

Let us assume that certain mode, say jth, lies in case i) so that $\left|X_j'(\lambda_j)\right| < 1$. Our goal is to find a bound of the error $\left|x_j^{(n)} - \lambda_j\right|$. From this inequality, there exists a radius $\delta > 0$ and certain $0 < \rho_j < 1$ such that

$$\left|X_j'(s)\right| \leq \rho_j < 1 \ , \ \forall \ s \in B(\lambda_j, \delta) = \{z \in \mathbb{C} : |z - \lambda_j| \leq \delta\}$$

Consider two any complex numbers inside this ball, $z_1, z_2 \in B(\lambda_j, \delta)$ and let us denote by $[z_1, z_2] = \{z_1(1 - t) + z_2\, t : 0 \leq t \leq 1\} \subset B(\lambda_j, \delta)$ to the straight segment connecting z_1 with z_2, then

$$|X_j(z_1) - X_j(z_2)| = \left|\int_{[z_1,z_2]} X_j'(s)\, \mathrm{d}s\right| = \left|\int_0^1 X_j'\left(s(\xi)\right)(z_1 - z_2)\, \mathrm{d}t\right| \leq \int_0^1 \left|X_j'\left(s(\xi)\right)\right| |z_1 - z_2|\, \mathrm{d}t \leq \rho_j\ |z_1 - z_2| \tag{44}$$

Since $0 < \rho_j < 1$, the function $X_j(s)$ is contractive in $B(\lambda_j, \delta)$; therefore, from the Banach's contraction principle the recursive sequence $x_j^{(n+1)} = X_j\left(x_j^{(n)}\right)$ will linearly converge to λ_j, for any starting point $x_j^{(0)} \in B(\lambda_j, \delta)$. Indeed, let $x_j^{(n+1)}, x_j^{(n)} \in B(\lambda_j, \delta)$ be two consecutive points of the previous sequence, then [33]

$$\left|x_j^{(n+1)} - x_j^{(n)}\right| = \left|X_j(x_j^{(n)}) - X_j(x_j^{(n-1)})\right| \leq \rho_j \left|x_j^{(n)} - x_j^{(n-1)}\right| \tag{45}$$

whence the linear convergence velocity is proved. Furthermore, the error in each iteration is bounded by [33]

$$\left|x_j^{(n)} - \lambda_j\right| \leq \frac{\rho_j^n}{1 - \rho_j}\left|X_j(x_j^{(0)}) - x_j^{(0)}\right| \tag{46}$$

As shown, in case of convergence, the velocity is inversely proportional to $|X'(\lambda_j)|$. Therefore, the numerical behavior of the recursive sequence and the physical characteristics of the damping model can be related provided that an analytical expression of $|X'(\lambda_j)|$ is available. At this end, let us consider λ_j, $\mathbf{u}_j$ any eigenpair of the original eigenproblem Eq. (3) and let $s = \lambda_j + ds$ be a small variation around λ_j. Expanding the s-functions and using the equalities $X_j(\lambda_j) = \lambda_j$ and $\boldsymbol{\mathcal{U}}_j(\lambda_j) = \mathbf{u}_j$, we obtain

$$\begin{aligned} X_j(s) &= X_j(\lambda_j + \mathrm{d}s) = X_j(\lambda_j) + X_j'(\lambda_j)\, \mathrm{d}s = \lambda_j + X_j'(\lambda_j)\, \mathrm{d}s \\ \boldsymbol{\mathcal{U}}_j(s) &= \boldsymbol{\mathcal{U}}_j(\lambda_j + \mathrm{d}s) = \boldsymbol{\mathcal{U}}_j(\lambda_j) + \boldsymbol{\mathcal{U}}_j'(\lambda_j)\, \mathrm{d}s = \mathbf{u}_j + \boldsymbol{\mathcal{U}}_j'(\lambda_j)\, \mathrm{d}s \\ \mathbf{G}(s) &= \mathbf{G}(\lambda_j + \mathrm{d}s) = \mathbf{G}(\lambda_j) + \mathbf{G}'(\lambda_j)\, \mathrm{d}s \end{aligned} \tag{47}$$

where $(\bullet)' = \mathrm{d}(\bullet)/\mathrm{d}s$. From Eqs. (34) and (37), it turns out that $z = X_j(s), Y_j(s)$ are the roots of the following second order polynomial equation in the variable z.

$$\frac{\boldsymbol{\mathcal{U}}_j^{\mathsf{H}}(s)\ \left[z^2\mathbf{M} + z\,\mathbf{G}(s) + \mathbf{K}\right]\ \boldsymbol{\mathcal{U}}_j(s)}{\boldsymbol{\mathcal{U}}_j^{\mathsf{H}}(s)\,\mathbf{M}\boldsymbol{\mathcal{U}}_j(s)} = 0 \tag{48}$$

Therefore, around the eigenvalue λ_j we can write for every $s = \lambda_j + \mathrm{d}s$

$$\boldsymbol{\mathcal{U}}_j^{\mathsf{H}}(s)\left[X_j^2(s)\mathbf{M} + X_j(s)\mathbf{G}(s) + \mathbf{K}\right]\boldsymbol{\mathcal{U}}_j(s) = 0 \tag{49}$$

Now, let us introduce the perturbed expressions obtained in Eq. (47)

$$\left(\mathbf{u}_j + \boldsymbol{\mathcal{U}}_j'(\lambda_j)\,\mathrm{d}s\right)^{\mathsf{H}} \Big[(\lambda_j + X'(\lambda_j)\,\mathrm{d}s)^2\,\mathbf{M} \\ + (\lambda_j + X'(\lambda_j)\,\mathrm{d}s)\,(\mathbf{G}(\lambda_j) + \mathbf{G}'(\lambda_j)\,\mathrm{d}s) + \mathbf{K}\Big] \left(\mathbf{u}_j + \boldsymbol{\mathcal{U}}_j'(\lambda_j)\,\mathrm{d}s\right) = 0 \quad (50)$$

Neglecting second order terms inside the brackets and rearranging

$$\left(\mathbf{u}_j + \boldsymbol{\mathcal{U}}_j'(\lambda_j)\,\mathrm{d}s\right)^{\mathsf{H}} \Big[\mathbf{D}(\lambda_j) + 2\lambda_j X'(\lambda_j)\mathbf{M}\,\mathrm{d}s + \lambda_j \mathbf{G}'(\lambda_j)\,\mathrm{d}s + X'(\lambda_j)\mathbf{G}(\lambda_j)\,\mathrm{d}s\Big] \left(\mathbf{u}_j + \boldsymbol{\mathcal{U}}_j'(\lambda_j)\,\mathrm{d}s\right) = 0 \quad (51)$$

where $\mathbf{D}(\lambda_j) = \lambda_j^2\mathbf{M} + \lambda_j\mathbf{G}(\lambda_j) + \mathbf{K}$ is the dynamic stiffness matrix evaluated at λ_j. Expanding the product of Eq. (51) the second order terms can again be neglected and also some terms vanish since $\mathbf{D}(\lambda_j)\,\mathbf{u}_j = \mathbf{0}$. Thus, after some simplifications Eq. (51) leads to

$$\left(2\lambda_j \mathbf{u}_j^{\mathsf{H}}\mathbf{M}\mathbf{u}_j + \mathbf{u}_j^{\mathsf{H}}\mathbf{G}(\lambda_j)\mathbf{u}_j\right) X_j'(\lambda_j) + \mathbf{u}_j^{\mathsf{H}}\mathbf{D}(\lambda_j)\boldsymbol{\mathcal{U}}_j'(\lambda_j) + \lambda_j \mathbf{u}_j^{\mathsf{H}}\mathbf{G}'(\lambda_j)\mathbf{u}_j = 0 \quad (52)$$

Finally, solving for $X_j'(\lambda_j)$

$$X_j'(\lambda_j) = -\frac{\mathbf{u}_j^{\mathsf{H}}\mathbf{D}(\lambda_j)\boldsymbol{\mathcal{U}}_j'(\lambda_j) + \lambda_j \mathbf{u}_j^{\mathsf{H}}\mathbf{G}'(\lambda_j)\mathbf{u}_j}{\mathbf{u}_j^{\mathsf{H}}\left[2\lambda_j\mathbf{M} + \mathbf{G}(\lambda_j)\right]\mathbf{u}_j} \quad (53)$$

Behind this expression we can find some interesting conclusions relating the local convergence of the proposed method with the nonproportionality and the nonviscousity of the system. At first view, we can detect two different terms in Eq. (53), say

$$NP_j = -\frac{\mathbf{u}_j^{\mathsf{H}}\mathbf{D}(\lambda_j)\boldsymbol{\mathcal{U}}_j'(\lambda_j)}{\mathbf{u}_j^{\mathsf{H}}\left[2\lambda_j\mathbf{M} + \mathbf{G}(\lambda_j)\right]\mathbf{u}_j}\ , \qquad NV_j = -\frac{\lambda_j \mathbf{u}_j^{\mathsf{H}}\mathbf{G}'(\lambda_j)\mathbf{u}_j}{\mathbf{u}_j^{\mathsf{H}}\left[2\lambda_j\mathbf{M} + \mathbf{G}(\lambda_j)\right]\mathbf{u}_j} \quad (54)$$

The notation is not arbitrary, because, as will be seen now, the first complex number is closely related to the nonproportionality of the damping model and the second to the nonviscousity or viscoelasticity, which represents the variation with frequency of the damping function. In general, we can not draw any conclusion *a priori* over the type of convergence around λ_j, because the Eq. (53) depends precisely on the mode of study. Only an analysis *a posteriori* would allow us to distinguish whether λ_j is an attractive or a repulsive fixed point. However, for some particular cases and under certain conditions, we can obtain approximate *a priori* results on the type of convergence.

4.1. Case 1: Light nonviscous damping

Let us see that indeed the term NP_j represents the effect of the nonproportionality in the velocity of convergence. This term involves, on one hand, the dynamical stiffness matrix $\mathbf{D}(\lambda_j)$ and, on the other hand, the complex vectors $\mathbf{u}_j$ and $\boldsymbol{\mathcal{U}}_j'(\lambda_j)$. From their definition —Eqs. (18),(33)—, both of them depend on the entrees of the offdiagonal terms of the damping matrix $\Gamma_{jk}(\lambda_j),\ j \neq k$ and on their derivatives $\Gamma_{jk}'(\lambda_j),\ j \neq k$. We can rewrite the expression of $\mathbf{u}_j$ from Eq. (18) and deduce from Eq. (29) a closed form expression for $\boldsymbol{\mathcal{U}}_j'(\lambda_j)$, after some straight math

$$\begin{aligned} \mathbf{u}_j &= \boldsymbol{\phi}_j + \boldsymbol{\Phi}_j\,\mathbf{a}_j = \boldsymbol{\phi}_j + \boldsymbol{\Phi}_j\,\left(\mathbf{P}_j - \mathbf{Q}_j\right)^{-1}\mathbf{g}_j & (55) \\ \boldsymbol{\mathcal{U}}_j'(s) &= \boldsymbol{\Phi}_j\,\boldsymbol{\alpha}_j'(s) = \boldsymbol{\Phi}_j\,\left[\boldsymbol{\mathcal{P}}_j(s) - \boldsymbol{\mathcal{Q}}_j(s)\right]^{-1}\boldsymbol{g}_j'(s) - \boldsymbol{\Phi}_j\,\left[\boldsymbol{\mathcal{P}}_j'(s) - \boldsymbol{\mathcal{Q}}_j'(s)\right]^{-1}\boldsymbol{g}_j(s) & (56) \end{aligned}$$

It will be consider that certain vector of $\mathbb{C}^N$ is of order r, say $\boldsymbol{\mathcal{O}}(r)$, if its components depend on the rth order of the entrees $\Gamma_{jk}(\lambda_j)$ and their s–derivatives. Thus, products of the type $\Gamma_{jk}(s)\Gamma_{lm}'(s)$ or $\Gamma_{jk}'(s)\Gamma_{lm}'(s)$ are considered as order $\boldsymbol{\mathcal{O}}(2)$ as well. Likewise, we will consider complex numbers of order r, denoted by $\mathcal{O}(r)$.

In Eq. (56), $\mathbf{\Phi}_j$ represents a $(N-1)\times N$ matrix with all undamped modes except the jth one. Therefore the following orthogonal relationships hold, $\boldsymbol{\phi}_j^{\mathsf{T}}\mathbf{M}\mathbf{\Phi}_j = \boldsymbol{\phi}_j^{\mathsf{T}}\mathbf{K}\mathbf{\Phi}_j = \mathbf{0}_{N-1}^{\mathsf{T}}$. In addition, from Eqs. (16) and (42), we have $\mathbf{a}_j = \boldsymbol{\mathcal{O}}(1)$ and $\boldsymbol{\alpha}_j'(\lambda_j) = \boldsymbol{\mathcal{O}}(1)$, and consequently we can write

$$\begin{aligned}
\mathbf{u}_j^{\mathsf{H}}\mathbf{D}(\lambda_j)\boldsymbol{\mathcal{U}}_j'(\lambda_j) &= \left(\boldsymbol{\phi}_j^{\mathsf{T}} + \mathbf{a}_j^{\mathsf{H}}\,\mathbf{\Phi}_j^{\mathsf{T}}\right)\left[\lambda_j^2\mathbf{M} + \lambda_j\mathbf{G}(\lambda_j) + \mathbf{K}\right]\left[\mathbf{\Phi}_j\,\boldsymbol{\alpha}_j'(\lambda_j)\right] \\
&= \lambda_j^2\mathbf{a}_j^{\mathsf{H}}\boldsymbol{\alpha}_j'(\lambda_j) + \lambda_j\mathbf{a}_j^{\mathsf{H}}\mathbf{\Phi}_j^{\mathsf{T}}\mathbf{G}(\lambda_j)\mathbf{\Phi}_j\boldsymbol{\alpha}_j'(\lambda_j) + \mathbf{a}_j^{\mathsf{H}}\left(\mathbf{\Phi}_j^{\mathsf{T}}\mathbf{K}\mathbf{\Phi}_j\right)\boldsymbol{\alpha}_j'(\lambda_j) \\
&= \mathcal{O}(2) + \mathcal{O}(3) + \mathcal{O}(2) = \mathcal{O}(2)
\end{aligned} \tag{57}$$

Although within NP_j also appear terms of the main diagonal $\Gamma_{kk}(\lambda_j)$ via the matrix $\mathbf{\Phi}_j^{\mathsf{T}}\mathbf{G}(\lambda_j)\mathbf{\Phi}_j$, they do in terms of order $\mathcal{O}(3)$ and additionally they are always affected by off–diagonal terms. Therefore, $NP_j \equiv 0$ holds for pure proportional systems and will become very small for light nonproportional damping due to the proved damping second–order dependency. In fact, this term does not appear in the derivations of Lázaro et al. [8] since only proportionally damped systems were considered.

Let us focus now on the nonviscousity term, NV_j. As shown in Eq. (54), it depends directly on the s–derivative of the damping matrix and represents the influence of the nonviscousity or viscoelasticity (rate of change of the damping model respect to the frequency). Expanding the value of $\mathbf{u}_j$ in the numerator of NV_j we have

$$\begin{aligned}
\mathbf{u}_j^{\mathsf{H}}\mathbf{G}'(\lambda_j)\mathbf{u}_j &= \left(\boldsymbol{\phi}_j^{\mathsf{T}} + \mathbf{a}_j^{\mathsf{H}}\,\mathbf{\Phi}_j^{\mathsf{T}}\right)\mathbf{G}'(\lambda_j)\left(\boldsymbol{\phi}_j + \mathbf{\Phi}_j\,\mathbf{a}_j\right) \\
&= \boldsymbol{\phi}_j^{\mathsf{T}}\mathbf{G}'(\lambda_j)\boldsymbol{\phi}_j + \boldsymbol{\phi}_j^{\mathsf{T}}\mathbf{G}'(\lambda_j)\mathbf{\Phi}_j\,\mathbf{a}_j + \mathbf{a}_j^{\mathsf{H}}\,\mathbf{\Phi}_j^{\mathsf{T}}\mathbf{G}'(\lambda_j)\boldsymbol{\phi}_j + \mathbf{a}_j^{\mathsf{H}}\,\mathbf{\Phi}_j^{\mathsf{T}}\mathbf{G}'(\lambda_j)\mathbf{\Phi}_j\,\mathbf{a}_j \\
&= \Gamma_{jj}'(\lambda_j) + \mathcal{O}(2) + \mathcal{O}(2) + \mathcal{O}(3) = \Gamma_{jj}'(\lambda_j) + \mathcal{O}(2)
\end{aligned} \tag{58}$$

Therefore, NV_j depends on the first order of the modal viscoelasticity. Plugging Eqs. (57) and (58) into Eq. (53)

$$X_j'(\lambda_j) = -\frac{\mathbf{u}_j^{\mathsf{H}}\mathbf{D}(\lambda_j)\boldsymbol{\mathcal{U}}_j'(\lambda_j) + \lambda_j\mathbf{u}_j^{\mathsf{H}}\mathbf{G}'(\lambda_j)\mathbf{u}_j}{\mathbf{u}_j^{\mathsf{H}}\left[2\lambda_j\mathbf{M} + \mathbf{G}(\lambda_j)\right]\mathbf{u}_j} = -\left[\mathcal{O}(2) + \lambda_j\Gamma_{jj}'(\lambda_j)\right]\left(\frac{1}{2\lambda_j} + \mathcal{O}(1)\right) = -\frac{\Gamma_{jj}'(\lambda_j)}{2} + \mathcal{O}(2) \tag{59}$$

Therefore the previous result is showing that the velocity of convergence of light nonviscously damped systems is mainly governed by the viscoelasticity. Moreover, we could approximate $X_j'(\lambda_j) \approx -\Gamma_{jj}'(\mathrm{i}\omega_j)/2$, expression which can be evaluated previously to the recursive process, providing valuable information on the velocity of convergence, for instance to predict the number of needed iterations to achieve a prefixed error.

4.2. Case 2: Light viscous damping

As known, viscous damping can be considered as a particular case of general nonviscously damped systemswhere

$$\boldsymbol{\mathcal{G}}(t) \equiv \mathbf{C}\,\delta(t) \quad , \quad \mathbf{G}(s) = \mathbf{C} \tag{60}$$

Therefore the damping coefficients do not depend on frequency and $\mathbf{G}'(s) \equiv \mathbf{0}$. Thus, the so–called nonviscous term NV_j taking part of $X_j'(\lambda_j)$ in Eq. (54) is null so that this latter can be evaluated as

$$X_j'(\lambda_j) = -\frac{\mathbf{u}_j^{\mathsf{H}}\mathbf{D}(\lambda_j)\boldsymbol{\mathcal{U}}_j'(\lambda_j)}{\mathbf{u}_j^{\mathsf{H}}\left[2\lambda_j\mathbf{M} + \mathbf{C}\right]\mathbf{u}_j} \tag{61}$$

Let us introduce the following notation for the modal damping matrix and its entrees

$$\boldsymbol{\mathcal{C}} = \mathbf{\Phi}^{\mathsf{T}}\,\mathbf{C}\,\mathbf{\Phi} \quad , \quad \mathcal{C}_{jk} = \boldsymbol{\phi}_j^{\mathsf{T}}\,\mathbf{C}\,\boldsymbol{\phi}_k \tag{62}$$

The matrix $\boldsymbol{\mathcal{C}}$ becomes diagonal only under certain mathematical conditions related to proportionality relationships between the damping matrix $\boldsymbol{\mathcal{C}}$ and the dynamic matrices $\mathbf{M}, \mathbf{K}$ [34, 30, 35]. In some cases of nonproportionality, the matrix $\boldsymbol{\mathcal{C}}$ is diagonally dominant but not purely diagonal, fact which is equivalent to assume as true

$$\sum_{\substack{k=1 \\ k\neq j}}^{N} |\mathcal{C}_{kj}| < |\mathcal{C}_{jj}| \ , \qquad \forall\ 1 \leq k, j \leq n \tag{63}$$

The system is then said to be *lightly nonproportional* or *nearly proportional*. Under this hypothesis, we can approximate the complex vectors $\mathbf{u}_j$ and $\boldsymbol{\mathcal{U}}_j(s)$ up to the first order in terms of the modal damping entrees —Eqs. (16),(43)— obtaining

$$\mathbf{u}_j \ \approx \ \boldsymbol{\phi}_j - \lambda_j \sum_{\substack{k=1 \\ k\neq j}}^{N} \frac{\mathcal{C}_{kj}}{d_k(\lambda_j)} \boldsymbol{\phi}_k \tag{64}$$

$$\boldsymbol{\mathcal{U}}_j(s) \ \approx \ \boldsymbol{\phi}_j - s \sum_{\substack{k=1 \\ k\neq j}}^{N} \frac{\mathcal{C}_{kj}}{d_k(s)} \boldsymbol{\phi}_k \tag{65}$$

where $d_k(s) = s^2 + s\,\mathcal{C}_{kk} + \omega_k^2$. Since for light damping we have $\lambda_j = \mathrm{i}\omega_j - \mathcal{C}_{jj}/2 + \mathcal{O}(2)$, we can expand the expression of $\mathbf{u}_j$ in terms of the modal damping parameters resulting in the well–known expression [36, 37]

$$\mathbf{u}_j \approx \boldsymbol{\phi}_j - \mathrm{i}\omega_j \sum_{\substack{k=1 \\ k\neq j}}^{N} \frac{\mathcal{C}_{kj}}{\omega_k^2 - \omega_j^2} \boldsymbol{\phi}_k \tag{66}$$

Something similar can be carried out on $\boldsymbol{\mathcal{U}}'_j(\lambda_j)$, after taking s–derivatives on Eq (65) and evaluating at $s = \lambda_j$. Thus, after some operations and simplifications we obtain

$$\boldsymbol{\mathcal{U}}'_j(\lambda_j) \approx -\sum_{\substack{k=1 \\ k\neq j}}^{N} \frac{\omega_k^2 + \omega_j^2}{\left(\omega_k^2 - \omega_j^2\right)^2} \mathcal{C}_{kj}\, \boldsymbol{\phi}_k \tag{67}$$

Now we plug Eqs. (66) and (67) into the numerator of Eq. (61) and expand the expression

$$\begin{aligned}
\mathbf{u}_j^{\mathsf{H}} \mathbf{D}(\lambda_j) \boldsymbol{\mathcal{U}}'_j(\lambda_j) \ &\approx \ \left[\boldsymbol{\phi}_j^{\mathsf{T}} + \mathrm{i}\omega_j \sum_{\substack{k=1 \\ k\neq j}}^{N} \frac{\mathcal{C}_{kj}}{\omega_k^2 - \omega_j^2} \boldsymbol{\phi}_k^{\mathsf{T}}\right] \left[\lambda_j^2 \mathbf{M} + \lambda_j \mathbf{C} + \mathbf{K}\right] \left[-\sum_{\substack{l=1 \\ l\neq j}}^{N} \frac{\omega_l^2 + \omega_j^2}{\left(\omega_l^2 - \omega_j^2\right)^2} \mathcal{C}_{lj}\, \boldsymbol{\phi}_l\right] \\
&= \ -\lambda_j^2 \sum_{\substack{l=1 \\ l\neq j}}^{N} \frac{\omega_l^2 + \omega_j^2}{\left(\omega_l^2 - \omega_j^2\right)^2} \mathcal{C}_{lj}\, \boldsymbol{\phi}_j^{\mathsf{T}} \mathbf{M}\, \boldsymbol{\phi}_l - \lambda_j \sum_{\substack{l=1 \\ l\neq j}}^{N} \frac{\omega_l^2 + \omega_j^2}{\left(\omega_l^2 - \omega_j^2\right)^2} \mathcal{C}_{lj}\, \boldsymbol{\phi}_j^{\mathsf{T}} \mathbf{C}\, \boldsymbol{\phi}_l \\
&\quad - \sum_{\substack{l=1 \\ l\neq j}}^{N} \frac{\omega_l^2 + \omega_j^2}{\left(\omega_l^2 - \omega_j^2\right)^2} \mathcal{C}_{lj}\, \boldsymbol{\phi}_j^{\mathsf{T}} \mathbf{K}\, \boldsymbol{\phi}_l - \mathrm{i}\omega_j\, \lambda_j^2 \sum_{\substack{k=1 \\ k\neq j}}^{N} \sum_{\substack{l=1 \\ l\neq j}}^{N} \frac{\mathcal{C}_{kj}\, \mathcal{C}_{lj}}{\omega_k^2 - \omega_j^2} \frac{\omega_l^2 + \omega_j^2}{\left(\omega_l^2 - \omega_j^2\right)^2} \boldsymbol{\phi}_k^{\mathsf{T}} \mathbf{M} \boldsymbol{\phi}_l \\
&\quad - \mathrm{i}\omega_j\, \lambda_j \sum_{\substack{k=1 \\ k\neq j}}^{N} \sum_{\substack{l=1 \\ l\neq j}}^{N} \frac{\mathcal{C}_{kj}\, \mathcal{C}_{lj}}{\omega_k^2 - \omega_j^2} \frac{\omega_l^2 + \omega_j^2}{\left(\omega_l^2 - \omega_j^2\right)^2} \boldsymbol{\phi}_k^{\mathsf{T}} \mathbf{C} \boldsymbol{\phi}_l - \mathrm{i}\omega_j \sum_{\substack{k=1 \\ k\neq j}}^{N} \sum_{\substack{l=1 \\ l\neq j}}^{N} \frac{\mathcal{C}_{kj}\, \mathcal{C}_{lj}}{\omega_k^2 - \omega_j^2} \frac{\omega_l^2 + \omega_j^2}{\left(\omega_l^2 - \omega_j^2\right)^2} \boldsymbol{\phi}_k^{\mathsf{T}} \mathbf{K} \boldsymbol{\phi}_l
\end{aligned} \tag{68}$$

Considering that $\lambda_j = \mathrm{i}\omega_j - \mathcal{C}_{jj}/2 + \mathcal{O}(2)$ and using the orthogonal relationships of Eq. (7) we obtain, after some straight simplifications

$$\mathbf{u}_j^{\mathsf{H}} \mathbf{D}(\lambda_j) \boldsymbol{\mathcal{U}}'_j(\lambda_j) = -2\mathrm{i}\omega_j \sum_{\substack{k=1 \\ k\neq j}}^{N} \frac{\omega_k^2 + \omega_j^2}{\left(\omega_k^2 - \omega_j^2\right)^2} \mathcal{C}_{kj}^2 \ + \ \mathcal{O}(3) \tag{69}$$

Using this expression, the derivative $X_j'(\lambda_j)$ for light viscous damping can be approximated by

$$
\begin{aligned}
X_j'(\lambda_j) \quad &= \quad -\frac{\mathbf{u}_j^{\mathsf{H}}\mathbf{D}(\lambda_j)\boldsymbol{\mathcal{U}}_j'(\lambda_j)}{\mathbf{u}_j^{\mathsf{H}}\left[2\lambda_j\mathbf{M}+\mathbf{C}\right]\mathbf{u}_j} = -\left[\frac{1}{2\mathrm{i}\omega_j}+\mathcal{O}(1)\right]\left[-2\mathrm{i}\omega_j\sum_{\substack{k=1\\k\neq j}}^{N}\frac{\omega_k^2+\omega_j^2}{\left(\omega_k^2-\omega_j^2\right)^2}\mathcal{C}_{kj}^2 \;+\; \mathcal{O}(3)\right] \\
&\approx \quad \sum_{\substack{k=1\\k\neq j}}^{N}\frac{\omega_k^2+\omega_j^2}{\left(\omega_k^2-\omega_j^2\right)^2}\mathcal{C}_{kj}^2
\end{aligned}
\tag{70}
$$

This expression is formed by a sum of squares of the off-diagonal elements of the damping matrix affected by the *distance* between the natural frequencies. Consequently, it reflects the close dependency between the nonproportionality of the system and the convergence velocity of the proposed numerical method. Moreover, it allows to establish *a priori* conditions for convergence for lightly damped viscous systems predicting with remarkable accuracy the value of $X_j'(\lambda_j)$, as will be shown in the numerical examples. Indeed, the recursive scheme will converge provided that

$$
\sum_{\substack{k=1\\k\neq j}}^{N}\frac{\omega_k^2+\omega_j^2}{\left(\omega_k^2-\omega_j^2\right)^2}\mathcal{C}_{kj}^2 < 1 \tag{71}
$$

Even more particular is the case of proportional viscous damping for which Eq. (70) vanishes. Hence, the identities $X_j'(s) = 0,\ X_j''(s) = 0, \ldots$ hold and the functions $X_j(s), Y_j(s)$ are constants and equal to the well–known jth complex modal eigenvalue, solution of the second order modal equation.

$$
\lambda_j = X_j(s) = -\zeta_j\omega_j + \mathrm{i}\omega_j\sqrt{1-\zeta_j^2}\ , \quad \lambda_j^* = Y_j(s) = -\zeta_j\omega_j - \mathrm{i}\omega_j\sqrt{1-\zeta_j^2}\ , \tag{72}
$$

where $\zeta_j = \mathcal{C}_{jj}/2\omega_j$.

4.3. Case 3: Overdamped viscous modes

Although in the introduction we have assumed that the eigenvalues set was only formed by conjugate–complex pairs, we will discuss the particular case of overdamped viscous modes since our derivative presents interesting properties. As known, overcritically damped modes are shown up for extremely high values of the damping parameters. They are characterized by negative real eigenvalues without oscillatory nature. Such cases are not usual in structures where energy dissipation is due to the intrinsic materials nature, but they could arise in systems with induced damping, like for instance artificial dampers. In general, the higher the damping the higher the real part of eigenvalues (in absolute value) and the lower the imaginary part, thought this is not general for all modes, but just for those most affected by the space distribution of the dampers). While the imaginary part does not vanish, the mode remains underdamped (oscillatory nature). For certain values of the damping coefficients within the matrix $\mathbf{C}$, the two conjugate–complex values of certain pair, say the jth one, merge into a double eigenvalue, whose value can be approximated by one of the natural frequencies, namely $\lambda_j \approx -\omega_j$, associated to the eigenvector $\boldsymbol{\phi}_j$ [38]. Exactly under this conditions the damping coefficients are said to be in a critical surface and the corresponding mode is said to be critically damped, resulting null simultaneously the two following approximated matrix equalities [38])

$$
\mathbf{D}(-\omega_j)\boldsymbol{\phi}_j \approx \mathbf{0} \quad , \quad \mathbf{D}'(-\omega_j)\boldsymbol{\phi}_j \approx \mathbf{0} \tag{73}
$$

where $\mathbf{D}'(s) = 2s\mathbf{M} + \mathbf{C}$ is the s–derivative of the dynamical stiffness matrix. If at this point, we keep increasing the damping, then the double root is branched in two simple negative real numbers. The modes associated to them are said to be overdamped. Let us denote by $\sigma_j \in \mathbb{R}^-$ to one of these overdamped eigenvalues and let us assume that it is fixed point of the function $X_j(s)$ (note that it is not known a priori what function among X_j and Y_j has any real eigenvalue as fixed point, something that do not happen for complex eigenvalues). Thus, we can obtain the associated eigenvector $\mathbf{x}_j \in \mathbb{R}^N$ so that

$$
\mathbf{D}(\sigma_j)\mathbf{x}_j = \mathbf{0} \quad , \quad \mathbf{D}'(\sigma_j)\mathbf{x}_j \neq \mathbf{0} \tag{74}
$$

The second inequality holds since we are not on a critical surface of the damping parameters. Therefore, according to Eq. (74) and using the properties of symmetry of the system matrices, the expression of $X_j'(\sigma_j)$ for any overdamped mode is

$$X_j'(\sigma_j) = -\frac{\mathbf{x}_j^{\intercal}\mathbf{D}(\sigma_j)\boldsymbol{\mathcal{U}}_j'(\sigma_j)}{\mathbf{x}_j^{\intercal}\left[2\lambda_j\mathbf{M}+\mathbf{C}\right]\mathbf{x}_j} = -\frac{\mathbf{x}_j^{\intercal}\mathbf{D}(\sigma_j)\boldsymbol{\mathcal{U}}_j'(\sigma_j)}{\mathbf{x}_j^{\intercal}\mathbf{D}'(\sigma_j)\mathbf{x}_j} = 0 \tag{75}$$

Thus result reveals a predicted quadratic convergence to real eigenvalues strictly overdamped. It is necessary to highlight that the convergence is locally quadratic, not globally. That means that there exist a boundary around σ_j within which the convergence is guaranteed and it will be very fast, expecting to achieve the same accuracy than that of a linear convergence but using much less iterations.

Let us see that the obtained result of Eq. (75) for overdamped modes (no critical) can not be extrapolated to those strictly critically damped. Indeed, assuming that $(\lambda_j, \mathbf{u}_j)$ forms an underdamped complex eigenpair, if now we vary the damping parameter getting close to a critical damping surface, then $\lambda_j \to -\omega_j$ y $\mathbf{u}_j \to \boldsymbol{\phi}_j$. Therefore,

$$\mathbf{D}(\lambda_j)\mathbf{u}_j \to \mathbf{D}(-\omega_j)\boldsymbol{\phi}_j \approx \mathbf{0} \quad , \quad \mathbf{D}'(\lambda_j)\mathbf{u}_j \to \mathbf{D}'(-\omega_j)\boldsymbol{\phi}_j \approx \mathbf{0} \tag{76}$$

which means that the expression of $X_j'(-\omega_j)$ becomes an indeterminate form. Abusing the notation, we have

$$X_j'(\lambda_j) \to X_j'(-\omega_j) = -\frac{\boldsymbol{\phi}_j^{\intercal}\mathbf{D}(-\omega_j)\boldsymbol{\mathcal{U}}_j'(-\omega_j)}{\boldsymbol{\phi}_j^{\intercal}\mathbf{D}'(-\omega_j)\boldsymbol{\phi}_j} \approx \frac{0}{0} = ? \tag{77}$$

A deep study of this limit depending on the damping conditions lies far from the aim of the present work. However, let us see that some qualitative conclusions of the behaviour of $X_j'(-\omega_j)$ can be drawn according to the value of $\boldsymbol{\mathcal{U}}_j'(-\omega_j)$, which as known is related to the nonproportionality of the system. Indeed, if the modes of the system, despite the high value of damping, are highly decoupled, then it is expected that $\boldsymbol{\mathcal{U}}_j'(-\omega_j)$ becomes very low, suggesting that the numerator could be one infinitesimal smaller than that of the denominator, resulting values of the derivative less than the unity. Otherwise, highly nonproportional systems could present local divergence, that is $\left|X_j'(-\omega_j)\right| > 1$. We would like to point out that this deduction is fruit of intuition and it is presented here just to try to find explanations at view of the numerical results. In order to provide more consistency to the proposed approach, we think that these conjectures could take part of future works together with the theoretical analysis of the limit (77).

The close relationship found between the level of damping, the level of viscoelasticity and the convergence of the system is shown in the numerical examples analyzed the next point.

5. Numerical examples

5.1. Example 1: Discrete system with nonviscous damping

In order to validate the obtained theoretical results, we analyze a 6–dof lumped-mass discrete system of Fig. 1. The mass and linear spring values are $m = 10^3$ kg, $k = 10^5$ N/m. Two different dampers are used to represent the dissipative model: a viscous damper joints the 3rd dof and the ground while a nonviscous damper is located between masses 4 and 5. The viscoelastic damper B is associated to a Biot's hereditary model with two exponential kernels. The damping functions for both dampers are

$$\begin{aligned} \mathcal{G}_A(t) &= \frac{c_A}{2}\left(\mu_1\,\mathrm{e}^{-\mu_1 t} + \mu_2\,\mathrm{e}^{-\mu_2 t}\right) \\ \mathcal{G}_B(t) &= c_B\;\delta(t) \end{aligned} \tag{78}$$

where c_A, c_B are the damping coefficients. As known [2], c_A is the parameter of the limit viscous damper when the relaxation parameters μ_1 and μ_2 tend to infinity. The damping ratios are $\zeta_A = c_A/2m\omega_0$, $\zeta_B =$

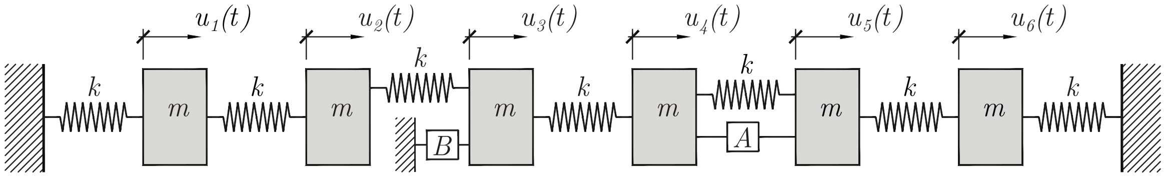

Figure 1: Examples 1 and 2: Lumped–mass dynamical system with viscous dampers. $k = 100$ kN/m, $m = 1$ t, $c_A = 2\omega_0\zeta_A$ and $c_B = 2\omega_0\zeta_A$, $\omega_0 = \sqrt{k/m}$

Table 2: Examples 1 and 2: Damping parameters and different cases of damping level.

		Damping parameters			
Example	Damping level	μ_1 (rad/s)	μ_2 (rad/s)	ζ_A	ζ_B
1. Non–viscous damping	Light damping (LD)	4.00	12.00	0.010	0.030
	High damping (HD)	4.00	12.00	1.200	0.800
2. Viscous damping	Light damping (LD)	∞	∞	0.009	0.007
	High damping (HD)	∞	∞	1.150	0.300

$c_B/2m\omega_0$, where $\omega_0 = \sqrt{k/m}$ is a reference frequency. The Laplace transforms of the damping functions are

$$\begin{aligned} G_A(s) &= \frac{c_A}{2}\left(\frac{\mu_1}{s+\mu_1} + \frac{\mu_2}{s+\mu_2}\right) = m\omega_0\zeta_A\left(\frac{\mu_1}{s+\mu_1} + \frac{\mu_2}{s+\mu_2}\right) \\ G_B(s) &= c_B = 2m\omega_0\zeta_B \end{aligned} \tag{79}$$

The damping matrix $\mathbf{G}(s)$ depends on the location of the dampers. Thus,

$$\mathbf{G}(s) = G_A(s)\mathbf{Q}_A + G_B(s)\mathbf{Q}_B \tag{80}$$

where

$$\mathbf{Q}_A = \begin{bmatrix} 0 & 0 & 0 & 0 & 0 & 0 \\ 0 & 0 & 0 & 0 & 0 & 0 \\ 0 & 0 & 0 & 0 & 0 & 0 \\ 0 & 0 & 0 & 1 & -1 & 0 \\ 0 & 0 & 0 & -1 & 1 & 0 \\ 0 & 0 & 0 & 0 & 0 & 0 \end{bmatrix}, \quad \mathbf{Q}_B = \begin{bmatrix} 0 & 0 & 0 & 0 & 0 & 0 \\ 0 & 0 & 0 & 0 & 0 & 0 \\ 0 & 0 & 1 & 0 & 0 & 0 \\ 0 & 0 & 0 & 0 & 0 & 0 \\ 0 & 0 & 0 & 0 & 0 & 0 \\ 0 & 0 & 0 & 0 & 0 & 0 \end{bmatrix}$$

Table 2 shows the assigned parameters for this example involving nonviscous damping, differentiating two cases respect to the damping level: light damping (LD) and high damping (HD).

We evaluate the eigenvalues sequences from Eqs. (39), although only the results of the recursion of function $X_j(s)$ will be shown, since those of $Y_j(s)$ are the conjugate–complex ones. Thus, we start each modal sequence from the undamped mode $x_j^{(0)} = \mathrm{i}\omega_j$ so that $x_j^{(n)} = X_j(x_j^{(n-1)})$, $n = 1, 2, \ldots$ —Eq. (38)—. According to the method, each step allows to obtain an eigenvector approximation, say $\mathbf{u}_j^{(n)} = \boldsymbol{\mathcal{U}}_j(x_j^{(n)})$ —Eq. (33)—. For each iteration, we can save the relative error between two consecutive values of the sequence, both for $\{x_j^{(n)}\}$ and $\{\mathbf{u}_j^{(n)}\}$, as

$$\epsilon_{x_j}^{(n)} = \frac{\left|x_j^{(n)} - x_j^{(n-1)}\right|}{\left|x_j^{(n-1)}\right|} \quad , \quad \epsilon_{\mathbf{u}_j}^{(n)} = \frac{\left\|\mathbf{u}_j^{(n)} - \mathbf{u}_j^{(n-1)}\right\|}{\left\|\mathbf{u}_j^{(n-1)}\right\|} \quad , \tag{81}$$

According to the Banach contraction principle, we have already shown in Eq. (46) that the error between the nth iteration and the exact eigenvalues is bounded by

$$\left|x_j^{(n)} - \lambda_j\right| \leq \frac{\rho_j^n}{1-\rho_j} \left|X_j(\mathrm{i}\omega_j) - \mathrm{i}\omega_j\right| \tag{82}$$

where $\rho_j = \max\{\left|X_j'(s)\right| : |s-\lambda_j| \leq \delta\} < 1$ is a bound of the derivative in certain ball centered at λ_j. Intuitively, it seems that the eigenvectors' sequence $\{\mathbf{u}_j^{(n)}\}$ converges provided that the eigenvalues's sequence also does. Let us see that this is true if the so–defined function $\boldsymbol{\mathcal{U}}_j'(s)$ is just bounded in the ball $B(\lambda_j, \delta)$. Indeed, let us assume that this bound exists and let us denote it by R_j, verifying

$$R_j \equiv \max_{|s-\lambda_j|\leq\delta} \left\|\boldsymbol{\mathcal{U}}_j'(s)\right\| \tag{83}$$

Then, $\boldsymbol{\mathcal{U}}_j(s)$ is Lipschitz continuous in $B(\lambda_j, \delta)$, so that

$$\|\boldsymbol{\mathcal{U}}_j(z_1) - \boldsymbol{\mathcal{U}}_j(z_2)\| \leq R_j \left|z_1 - z_2\right| \ , \quad \forall\, z_1, z_2 \in B(\lambda_j, \delta) \tag{84}$$

Let us assume that the result of the nth iteration lies inside the ball $B(\lambda_j, \delta)$, i.e. $x_j^{(n)} \in B(\lambda_j, \delta)$. Using Eqs. (84) and (82), the distance between the nth element of the sequence, $\mathbf{u}_j^{(n)}$, and the jth exact eigenvector $\mathbf{u}_j$ can be bounded by

$$\left\|\mathbf{u}_j^{(n)} - \mathbf{u}_j\right\| = \left\|\boldsymbol{\mathcal{U}}_j(x_j^{(n)}) - \boldsymbol{\mathcal{U}}_j(\lambda_j)\right\| \leq R_j \left|x_j^{(n)} - \lambda_j\right| \leq \frac{R_j\, \rho_j^n}{1-\rho_j} \left|X(\mathrm{i}\omega_j) - \mathrm{i}\omega_j\right| \tag{85}$$

which in addition shows the linear rate of convergence of $\{\mathbf{u}_j^{(n)}\}$ up to the jth eigenvector $\mathbf{u}_j$, provided that R_j exists. These theoretical derivations are in agreement with the results of the numerical example, as will be described now in the Table 3 and Fig. 2.

Table 3: Example 1: Numerical results for Nonviscous damping. Light damping case (LD) top, High damping case (HD) bottom. Eigenvectors are listed in Table 4

EXAMPLE 1. NONVISCOUS LIGHT DAMPING

Mode	Q-factor	Iterations	Sequence Limit	$X(s)$–derivative	
j	Q_j	$n_{\max}$	$x_j^{(n_{\max})}$	$\lvert X'(\lambda_j)\rvert$	$\lvert\Gamma'_{jj}(\lambda_j)\rvert /2$
1	76.18	6	$-0.0292200 + 4.4518011i$	0.00032	0.00026
2	283.67	7	$-0.0153141 + 8.6884111i$	0.00117	0.00108
3	118.26	8	$-0.0529305 + 12.5191688i$	0.00373	0.00364
4	404.77	6	$-0.0193199 + 15.6404084i$	0.00022	0.00022
5	266.20	8	$-0.0339477 + 18.0740492i$	0.00395	0.00299
6	137.86	8	$-0.0710403 + 19.5871733i$	0.00541	0.00414

EXAMPLE 1. NONVISCOUS HIGH DAMPING

Mode	Q-factor	Iterations	Sequence Limit	$X(s)$–derivative	
j	Q_j	$n_{\max}$	$x_j^{(n_{\max})}$	$\lvert X'(\lambda_j)\rvert$	$\lvert\Gamma'_{jj}(\lambda_j)\rvert /2$
1	0.03	345	$-10.9717211 + 0.6264562i$	0.91354	0.52636
2	4.36	194	$-1.0521580 + 9.1689969i$	0.85433	0.03021
3	2.62	154	$-1.6460262 + 8.6163849i$	0.81052	0.19824
4	19.36	30	$-0.3888621 + 15.0563065i$	0.31863	0.00637
5	24.79	25	$-0.3505189 + 17.3789321i$	0.25112	0.09358
6	5.59	24	$-2.0847565 + 23.2949098i$	0.16616	0.09702

The Table 3 shows the main numerical results of this example. In the second column modal quality factors are listed. This parameter is commonly used to measure the modal damping level of the jth mode. Its mathematical definition depends on the relationship between the imaginary part and real part of the eigenvalue

$$Q_j = -\frac{\Im\{s_j\}}{2\Re\{s_j\}} \tag{86}$$

Since the damping model induces a strictly dissipative motion, $\Re\{s_j\} < 0$, for $1 \leq j \leq 6$, hence the negative sign in the definition. The exponential decay of amplitudes is directly related to the real part of eigenvalues, therefore the lower Q_j, the higher the modal damping level. Woodhouse [36] considers $Q_j \leq 10$ "as very high damping for most structural vibration applications". Moreover, overdamped modes verify $Q_j = 0$. Otherwise, the upper bound $Q_j = \infty$ characterizes an undamped mode. The values of Q_j in the Table 3, allow to observe in a fast sight what modes are more affected by the dissipative model. In the third column, the value $n_{\max}$ represents the number of iterations needed for achieving an error of $\epsilon_{x_j}^{(n)} \leq 10^{-15}$. According to the convergence analysis, the derivative of the recursive function evaluated at the eigenvalue contains valuable information on the velocity of convergence. Moreover, this latter can be approximated by $\left|X_j'(\lambda_j)\right| \approx \Gamma'_{jj}(\lambda_j)/2$ for lightly damped systems. Both results are listed for each mode in columns 5th and 6th. As expected, highly damped case shows a lack of accuracy in this approximation. Setting any mode and comparing light and high damping cases, we observe a clear relationship between the level of damping, the number of needed iterations and the value of $\left|X_j'(\lambda_j)\right|$, so that the higher the damping, the closer to the unity is the derivative and also the greater number of required iterations. As result of the iterative process the damped eigenvectors obtained after convergence are shown as well in Table 4

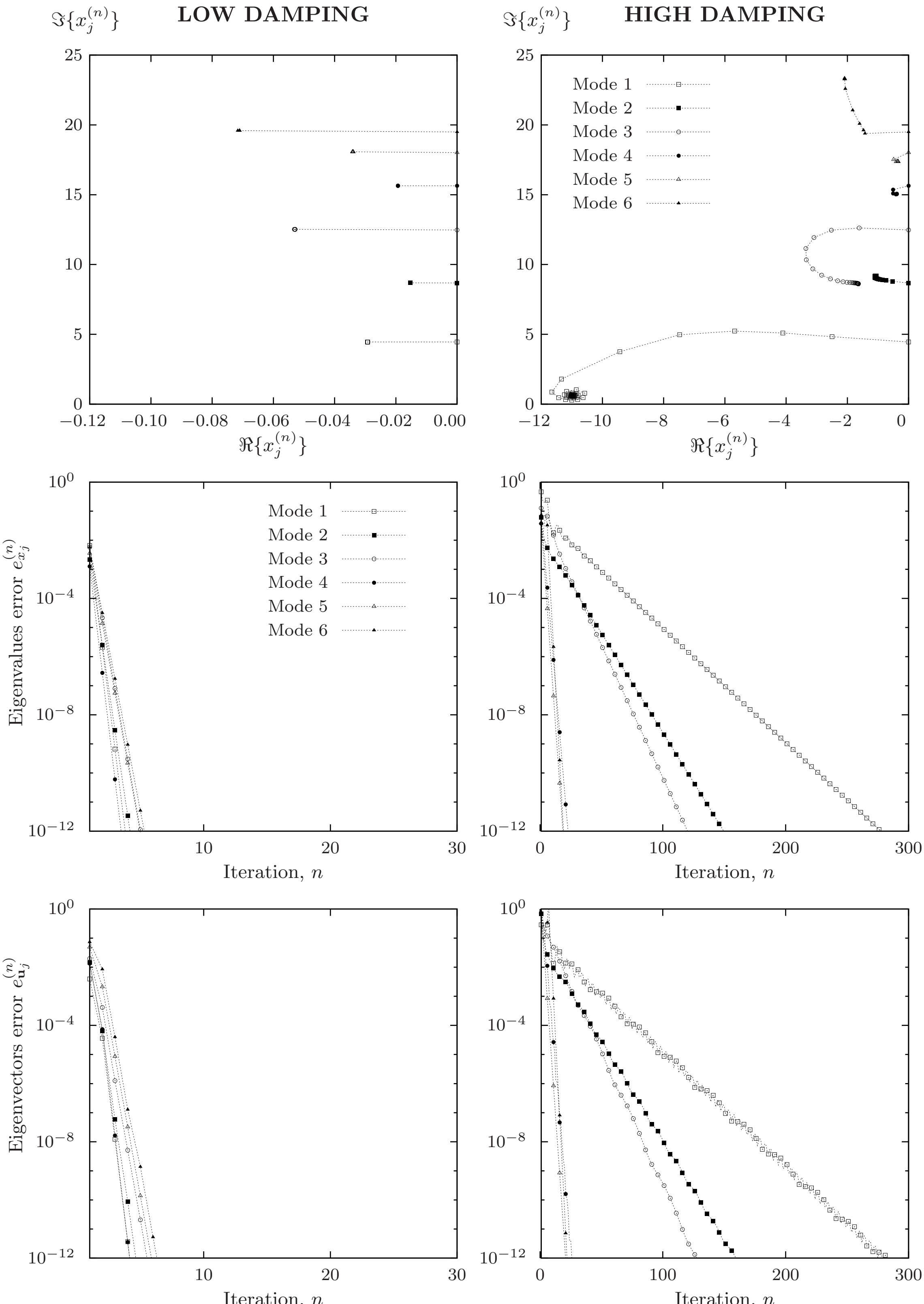

Figure 2: Example 1: Nonviscous damping. Top plots: sequences' paths in the complex plane in rad/s. Middle plots, iteration error of the eigenvalues sequences. Bottom plots: iteration of the eigenvectors sequences

In the Fig. 2 the iterative process is shown graphically. Both LD and HD cases are represented in the left and right plots, respectively. The level of damping of the both cases considered can be clearly observed in the scale of the real part (top figures). As expected, the damping level strongly affects to the velocity of convergence. Moreover, we can observe the predicted linear decay of the iteration error (observed with logarithmic scale of the ordinate axis) for all modes. The slope of the error–decay is closely related to the value of $\left|X_j'(\lambda_j)\right|$ as shown in the Table 3. And, in turn, this latter increases with the level of the nonproportionality and the viscoelasticity in the system, as demonstrated in Eqs. (53) and (54). As proved in Eq. (85), also the recursive process of the eigenvectors' sequence obey to a linear scheme, as can be seen in bottom plots.

Table 4: Numerical results of damped eigenvectors after the convergence of the iterative process, for nonviscous damping (Example 1) and viscous damping (Example 2)

EXAMPLE 1. NON–VISCOUS LIGHT DAMPING EIGENVECTORS

Mode, j	u_{j1}	u_{j2}	u_{j3}	u_{j4}	u_{j5}	u_{j6}
$\mathbf{u}_1^{(n_{\max})}$	$0.232 - 0.000i$	$0.418 - 0.001i$	$0.521 - 0.002i$	$0.521 - 0.000i$	$0.419 + 0.003i$	$0.232 + 0.002i$
$\mathbf{u}_2^{(n_{\max})}$	$0.420 - 0.000i$	$0.523 - 0.001i$	$0.231 - 0.003i$	$-0.235 + 0.001i$	$-0.518 + 0.011i$	$-0.416 + 0.008i$
$\mathbf{u}_3^{(n_{\max})}$	$0.522 - 0.000i$	$0.226 - 0.007i$	$-0.424 - 0.006i$	$-0.409 - 0.001i$	$0.228 - 0.003i$	$0.527 + 0.010i$
$\mathbf{u}_4^{(n_{\max})}$	$0.518 - 0.000i$	$-0.231 - 0.003i$	$-0.415 + 0.003i$	$0.416 - 0.009i$	$0.235 + 0.002i$	$-0.527 + 0.003i$
$\mathbf{u}_5^{(n_{\max})}$	$0.428 - 0.000i$	$-0.542 - 0.005i$	$0.258 + 0.013i$	$0.214 - 0.005i$	$-0.503 + 0.004i$	$0.397 - 0.007i$
$\mathbf{u}_6^{(n_{\max})}$	$0.213 - 0.000i$	$-0.391 - 0.006i$	$0.505 + 0.022i$	$-0.537 - 0.028i$	$0.444 + 0.025i$	$-0.242 - 0.010i$

EXAMPLE 1. NON–VISCOUS HIGH DAMPING EIGENVECTORS

Mode, j	u_{j1}	u_{j2}	u_{j3}	u_{j4}	u_{j5}	u_{j6}
$\mathbf{u}_1^{(n_{\max})}$	$0.096 - 0.000i$	$0.308 - 0.013i$	$0.886 - 0.085i$	$0.196 - 0.023i$	$0.242 + 0.016i$	$0.075 + 0.008i$
$\mathbf{u}_2^{(n_{\max})}$	$0.503 - 0.000i$	$0.589 - 0.097i$	$0.167 - 0.227i$	$0.021 + 0.225i$	$0.012 + 0.389i$	$-0.043 + 0.326i$
$\mathbf{u}_3^{(n_{\max})}$	$0.385 - 0.000i$	$0.494 - 0.109i$	$0.219 - 0.280i$	$0.201 + 0.251i$	$0.220 + 0.428i$	$0.093 + 0.354i$
$\mathbf{u}_4^{(n_{\max})}$	$0.146 - 0.000i$	$-0.039 - 0.017i$	$-0.138 + 0.009i$	$0.057 - 0.469i$	$0.145 - 0.190i$	$-0.194 + 0.800i$
$\mathbf{u}_5^{(n_{\max})}$	$0.682 - 0.000i$	$-0.695 - 0.083i$	$0.016 + 0.169i$	$-0.008 - 0.039i$	$-0.022 - 0.081i$	$0.031 + 0.076i$
$\mathbf{u}_6^{(n_{\max})}$	$0.010 - 0.000i$	$-0.034 - 0.010i$	$0.097 + 0.067i$	$-0.649 + 0.197i$	$0.654 - 0.240i$	$-0.160 + 0.117i$

EXAMPLE 2. VISCOUS LIGHT DAMPING EIGENVECTORS

Mode, j	u_{j1}	u_{j2}	u_{j3}	u_{j4}	u_{j5}	u_{j6}
$\mathbf{u}_1^{(n_{\max})}$	$0.232 - 0.000i$	$0.418 - 0.001i$	$0.521 - 0.002i$	$0.521 + 0.000i$	$0.418 + 0.002i$	$0.232 + 0.001i$
$\mathbf{u}_2^{(n_{\max})}$	$0.418 - 0.000i$	$0.521 - 0.001i$	$0.232 - 0.002i$	$-0.232 + 0.002i$	$-0.521 + 0.008i$	$-0.418 + 0.006i$
$\mathbf{u}_3^{(n_{\max})}$	$0.521 - 0.000i$	$0.232 - 0.006i$	$-0.418 - 0.005i$	$-0.418 - 0.001i$	$0.232 - 0.002i$	$0.521 + 0.009i$
$\mathbf{u}_4^{(n_{\max})}$	$0.521 - 0.000i$	$-0.232 - 0.003i$	$-0.418 + 0.003i$	$0.418 - 0.008i$	$0.232 + 0.002i$	$-0.521 + 0.001i$
$\mathbf{u}_5^{(n_{\max})}$	$0.418 - 0.000i$	$-0.521 - 0.007i$	$0.232 + 0.017i$	$0.232 - 0.010i$	$-0.521 + 0.011i$	$0.417 - 0.015i$
$\mathbf{u}_6^{(n_{\max})}$	$0.232 - 0.000i$	$-0.418 - 0.008i$	$0.520 + 0.028i$	$-0.519 - 0.042i$	$0.416 + 0.040i$	$-0.231 - 0.018i$

EXAMPLE 2. VISCOUS HIGH DAMPING EIGENVECTORS

Mode, j	u_{j1}	u_{j2}	u_{j3}	u_{j4}	u_{j5}	u_{j6}
$\mathbf{u}_1^{(n_{\max})}$	$0.081 - 0.000i$	$0.281 - 0.000i$	$0.897 - 0.000i$	$0.330 - 0.000i$	$0.036 - 0.000i$	$0.010 - 0.000i$
$\mathbf{u}_2^{(n_{\max})}$	$0.319 - 0.000i$	$0.430 - 0.069i$	$0.246 - 0.187i$	$0.138 + 0.283i$	$0.139 + 0.562i$	$0.035 + 0.422i$
$\mathbf{u}_3^{(n_{\max})}$	$0.564 - 0.000i$	$0.619 - 0.124i$	$0.087 - 0.272i$	$-0.007 + 0.071i$	$0.071 + 0.324i$	$0.005 + 0.296i$
$\mathbf{u}_4^{(n_{\max})}$	$0.148 - 0.000i$	$-0.053 - 0.034i$	$-0.136 + 0.024i$	$0.045 - 0.431i$	$0.321 - 0.120i$	$-0.487 + 0.642i$
$\mathbf{u}_5^{(n_{\max})}$	$0.682 - 0.000i$	$-0.695 - 0.085i$	$0.015 + 0.173i$	$0.008 - 0.046i$	$-0.051 - 0.065i$	$0.057 + 0.057i$
$\mathbf{u}_6^{(n_{\max})}$	$0.060 - 0.000i$	$-0.031 - 0.120i$	$-0.283 + 0.124i$	$0.325 - 0.650i$	$-0.196 + 0.500i$	$-0.211 - 0.153i$

5.2. Example 2: Discrete system with viscous damping

Let us consider the same 6–dof discrete system of Fig. (1) but assuming purely viscous dampers. Thus, the hereditary damping functions can be written as

$$\begin{aligned} \mathcal{G}_A(t) &= c_A\ \delta(t) \\ \mathcal{G}_B(t) &= c_B\ \delta(t) \end{aligned} \tag{87}$$

and the constant damping matrix is

$$\mathbf{C} = c_A\mathbf{Q}_A + c_B\mathbf{Q}_B \tag{88}$$

One of the reason of designing a numerical example based on viscous damping is to compare the value of the modal convergence parameter $\left|X_j'(\lambda_j)\right|$. According to the shown theory, the major difference between lightly damped nonviscous and viscous systems is a term specifically associated to the viscoelasticity and approximated by $\Gamma_{jj}'(\lambda_j)/2$. For this reason we try to assign values of the damping ratios, ζ_A and ζ_B so that the quality factor remain approximately constant between examples 1 and 2. The values of damping rations for this example are shown in Table 2. This allows us to draw conclusions and check the effect of the viscoelasticity in the velocity of convergence. For instance, taking the third mode, the quality factor for the examples 1 and 2 (LD cases) are $Q_3 \approx 118$ (example 1) and $Q_3 \approx 138$ (example 2). In terms of the value of $\left|X_j'(\lambda_j)\right|$, the nonviscous derivative is almost 15 times higher than that of the viscous example, something similar to the expected value from the theoretical results, which predicted that both values differ in one order of magnitude (Eqs. (59)). We note also the effect in the convergence due to the relative distance between natural frequencies. In Table 5, LD case and modes 5th and 6th, we see that the natural frequencies are very close: $\omega_5 \approx 18.02$ rad/s and $\omega_6 \approx 19.49$ rad/s. According to Eq. (70), this directly affects to the corresponding values of $X_j'(\lambda_j)$ increasing them respect to those of the rest of modes.

It is worthy to highlight the remarkable accuracy of the approximation of $X_j'(\lambda_j)$ in Eq. (70) derived for lightly damped systems, which is shown (together with the exact values) in the two last columns of Table 5 (light damping case). This validates the use of Eq. (70) as a first estimation of the rate of decay of the error in each iteration por lightly damped systems.

Table 5: Example 2: Numerical results for Viscous damping. Light damping case (LD) top, High damping case (HD) bottom. Eigenvectors are listed in Table 4

EXAMPLE 2. VISCOUS LIGHT DAMPING

Mode	Q-factor	Iterations	Sequence Limit	X–derivative	
j	Q_j	$n_{\max}$	$x_j^{(n_{\max})}$	$\lvert X'(\lambda_j)\rvert$	$\sum_{\substack{k=1\\k\neq j}}^{N} \frac{\omega_k^2+\omega_j^2}{\left(\omega_k^2-\omega_j^2\right)^2}\,\mathcal{C}_{kj}^2$
1	88.35	6	$-0.0251876 + 4.4504418\mathrm{i}$	0.5802E-04	0.5802E-04
2	405.70	6	$-0.0106949 + 8.6777536\mathrm{i}$	1.0224E-04	1.0225E-04
3	137.69	6	$-0.0452812 + 12.4698028\mathrm{i}$	2.4839E-04	2.4842E-04
4	431.13	6	$-0.0181348 + 15.6367835\mathrm{i}$	1.5652E-04	1.5659E-04
5	202.37	7	$-0.0445211 + 18.0198078\mathrm{i}$	15.0407E-04	15.0425E-04
6	113.12	7	$-0.0861803 + 19.4968932\mathrm{i}$	15.3067E-04	15.3087E-04

EXAMPLE 2. VISCOUS HIGH DAMPING

Mode	Q-factor	Iterations	Sequence Limit	X–derivative	
j	Q_j	$n_{\max}$	$x_j^{(n_{\max})}$	$\lvert X'(\lambda_j)\rvert$	$\sum_{\substack{k=1\\k\neq j}}^{N} \frac{\omega_k^2+\omega_j^2}{\left(\omega_k^2-\omega_j^2\right)^2}\,\mathcal{C}_{kj}^2$
1	0.00	11	$-12.1484799 + 0.0000000\mathrm{i}$	0.0000	0.8124
2	3.07	264	$-1.3322435 + 8.1778897\mathrm{i}$	0.8841	0.7634
3	4.17	453	$-1.1477300 + 9.5721253\mathrm{i}$	0.9303	1.6970
4	10.41	25	$-0.7389033 + 15.3792946\mathrm{i}$	0.2390	2.1285
5	24.28	21	$-0.3579261 + 17.3785089\mathrm{i}$	0.1900	1.1888
6	1.44	26	$-5.8852486 + 16.9224333\mathrm{i}$	0.1977	1.8592

In this example and for the high damping case the damping parameters have been modified in order to obtain an overdamped mode (mode 1 of Table 5, HD case). The convergence parameter verifies $|X_1'(\lambda_1)| = 0$ and the quadratic velocity of convergence can be noted from the number of iterations. In this case, the recursive sequence after few iterations, remains inside the real numbers up to converge at the eigenvalue (see Fig. 3, HD case). The dissipative model affects the convergence velocity specially in modes 2nd and 3rd, which present values of the convergence parameter close to the unity and a number of iterations notably higher than those of the other modes.

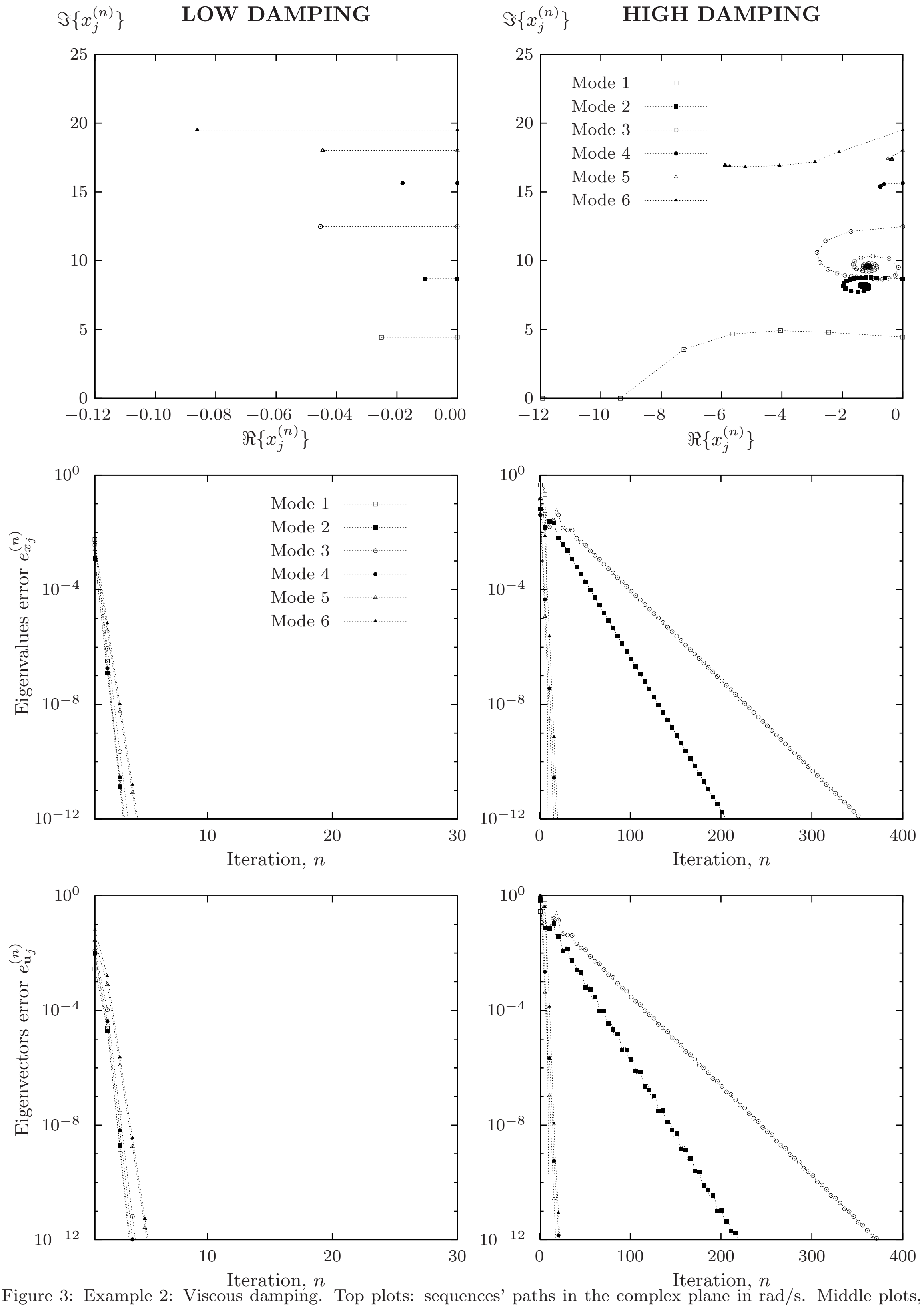

Figure 3: Example 2: Viscous damping. Top plots: sequences' paths in the complex plane in rad/s. Middle plots, iteration error of the eigenvalues sequences. Bottom plots: iteration of the eigenvectors sequences

In Fig. 4 the frequency response function relating the dof's 2 and 6 is shown for the examples 1 and 2 (discrete system), representing in the same plot the different damping cases, both in absolute value and phase. From the comparison of these curves, the two levels of damping considered can be graphically visualized.

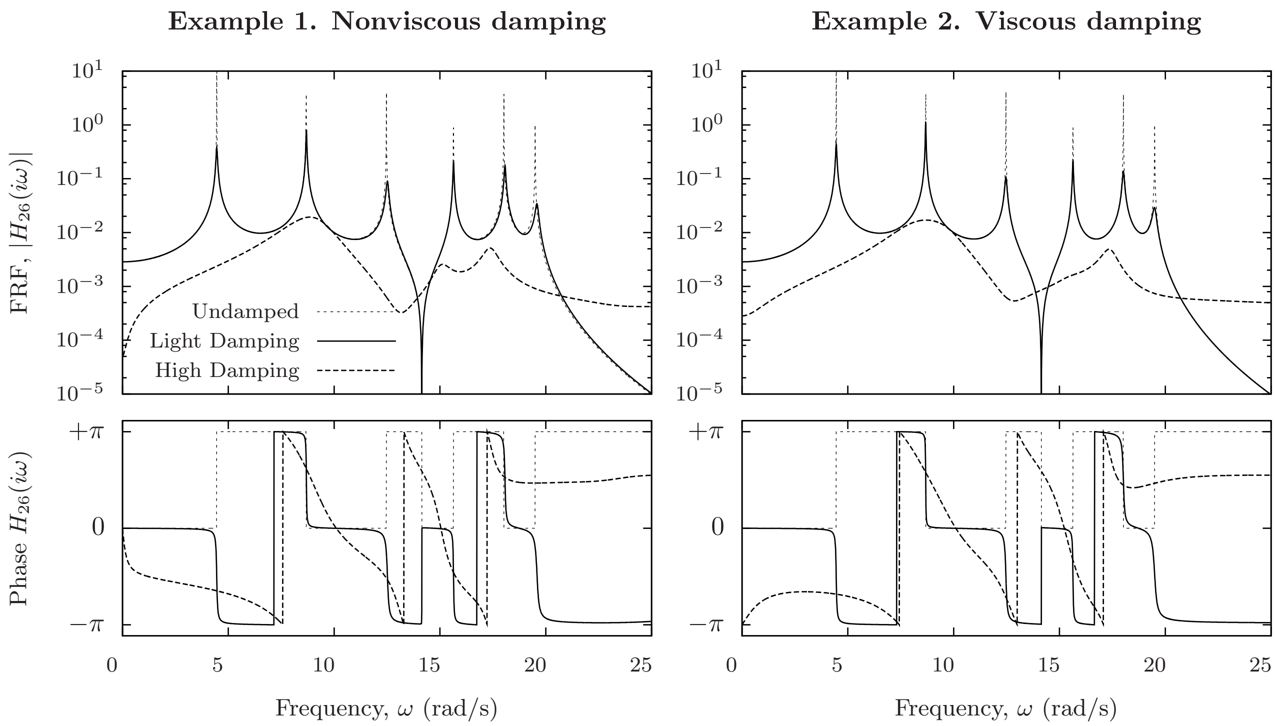

Figure 4: Frequency Response Function $H_{26}(\mathrm{i}\omega)$ for Examples 1 and 2

In addition to the shown examples for discrete systems, we have checked the numerical method for other several cases in order to investigate the behavior of the sequences. The scheme always starts using the natural frequencies as initial guesses, that is $x_j^{(0)} = \mathrm{i}\omega_j$. So that initially we have six different sequences. In general, we have found out that the six iterative processes always convergence even for highly damped systems, although for some cases two or more sequences finished the process at the same mode. This fact can be due to two reasons: (i) two complex eigenvalues lie very close one each other, so that one of them presents more attractive power. Or, mathematically, its convergence parameter $\left|X_j'(\lambda_j)\right|$ is much lower. (ii) one eigenvalue could be repulsive, that is $\left|X_j'(\lambda_j)\right| > 1$, so that the sequence automatically is attracted by the closest mode. These scenarios have been detected for extremely damped systems, which in general lie far from the majority of physical systems used for engineering applications.

5.3. Example 3: Continuous Discrete system with viscous damping

In this last example the proposed method will be validated for continuous systems. For that a cantilever beam of length $l = 5$ m with a local viscoelastic support is considered (see Fig. 5). The material of the beam is steel with Young modulus $E = 210$ GPa and density $\rho = 7.85$ t/m^3. The cross section is constant with a flexural stiffness of $EI = 224$ kNm^2 and a mass per unit of length of $\rho A = 0.0628$ t/m. The damper located at the right edge has a local stiffness of $k_D = 0.2EI/l^3 = 0.3584$ kN/m and a viscoelastic damping

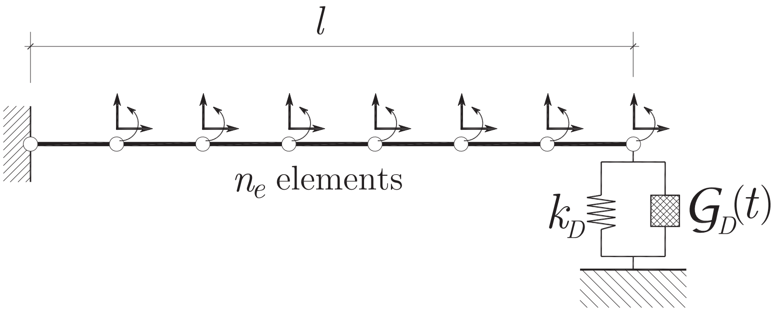

Figure 5: Example 3: Continuous system formed by a beam modeled with n_e two–nodes finite elements (three degrees of freedom per node). A local nonviscous damper is located under the right edge.

function in time and frequency domain defined by

$$\begin{aligned} \mathcal{G}_D(t) &= \frac{c_D}{2}\left(\mu_1\, \mathrm{e}^{-\mu_1 t} + \mu_2\, \mathrm{e}^{-\mu_2 t}\right) \\ G_D(s) &= \frac{c_D}{2}\left(\frac{\mu_1}{s+\mu_1} + \frac{\mu_2}{s+\mu_2}\right) = m\omega_0\zeta_D\left(\frac{\mu_1}{s+\mu_1} + \frac{\mu_2}{s+\mu_2}\right) \end{aligned} \tag{89}$$

where $\zeta_D = c_D/2m\omega_0$ represents the damping ratio, $m = 0.314$ t is the total mass of the beam and $\omega_0 = \sqrt{EI/ml^3} = 2.3889$ rad/s is the reference frequency. For this example the value of the damping ratio is $\zeta_D = 0.50$. The values of the relaxation parameters are $\mu_1 = 4$ rad/s and $\mu_2 = 12$ rad/s. The beam is modeled using n_e two-nodes Euler-Bernoulli finite elements. Each node has three degrees of freedom (two displacements and rotation). Therefore the structural model has a total number of $N = 3n_e$ free degrees of freedom. The main objective of this example is to evaluate the behavior of the proposed method as the number of degrees of freedom increases. In particular, how afects the parameter N (total number of dofs) to the number of iterations for convergence. Thus, setting an iteration error in $\epsilon_{\max} = 10^{-5}$ the number of the required iterations until getting this error is listed in Table 6 for the six first modes of the beam. As observed, the number of iterations remains constant and is not affected by the number of degrees of freedom. This result can be predicted by the developed theoretical results on the convergence since the number of iterations is close related to the derivative $\left|X_j'(\lambda_j)\right|$ and this latter, as proved, depends on the type of damping, on how strong is that damping and on the level of nonproportionality (damping distribution along the structure).

Table 6: Example 3: Number of required iterations until convergence for different mesh sizes. n_e is the number of finite elements, $N = 3n_e$ is the number of degrees of freedom

Mode, j	Q-factor, Q_j	$n_e = 10$ $N = 30$	$n_e = 50$ $N = 150$	$n_e = 200$ $N = 600$	$n_e = 350$ $N = 1050$
1	3.17E+00	11	11	11	11
2	1.99E+02	5	5	5	5
3	4.19E+03	4	4	4	4
4	3.15E+04	4	4	4	4
5	1.42E+05	4	4	4	4
6	4.74E+05	3	3	3	3

It is expected that the bigger the system, the higher the computational cost. However, this increasing of computation time does not come from a higher number of iterations but from the amount of time required to solve the s-dependent vector $\boldsymbol{\mathcal{U}}_j(s)$ from Eq. (33) in every iteration. As seen, $\boldsymbol{\mathcal{U}}_j(s)$ arises from the solution of a linear system of size $N-1$ which, as known, requires a number of operations of order $\mathcal{O}\left((N-1)^3\right)$. At the end of the iterative process, this system will have been solved as many times as the number of required iterations until the imposed error. If the system is lightly damped, with two or three iterations we will obtain very accurate results even if the system has thousands of degrees of freedom. For these systems the expression of $\boldsymbol{\mathcal{U}}_j(s)$ derived from the Neuman series expansion —Eq. (43)— could be more suitable since does not require solving a linear system, allowing us to reduce even more the computational cost.

As a final note, we describe a procedure to accelerate the rate of convergence of our recursive sequences from linear to quadratic proposed by Aitken [39] and known as *Aitken's delta-squared process*. This simple implementation does not increase the computational effort and allows this method to compete with those based on Newton–Raphson schemes with a known quadratic convergence. Indeed, for any iterative sequence converging linearly, say $\{x_j^{(n)}\}$, we can always build another sequence, say $\{w_j^{(n)}\}$ which converges quadratically to the same limit. The nth term $w_j^{(n)}$ is evaluated as

$$w_j^{(n)} = \frac{x_j^{(n+2)}\, x_j^{(n)} - \left(x_j^{(n+1)}\right)^2}{x_j^{(n+2)} - 2x_j^{(n+1)} + x_j^{(n)}} \tag{90}$$

The name delta–squared process comes from the alternative form which can adopts the above expression, say

$$w_j^{(n)} = x_j^{(n)} - \frac{\left(\Delta x_j^{(n)}\right)^2}{\Delta^2 x_j^{(n)}} \tag{91}$$

where $\Delta x_j^{(n)} = x_j^{(n+1)} - x_j^{(n)}$ and $\Delta^2 x_j^{(n)} = \Delta x_j^{(n+1)} - \Delta x_j^{(n)} = x_j^{(n+2)} - 2x_j^{(n+1)} + x_j^{(n)}$. This improvement in the method can be specially useful for highly damped nonproportional systems since the number of iterations can notably be reduced.

6. Conclusions

Vibrating systems are governed by the well–known dynamical equilibrium equations involving inertial, dissipative and stiffness forces. In the most general case, damping forces can be modeled by the so–called nonviscous models considering those forces as depending on the time history of the degrees of freedom via hereditary kernel functions. The dynamic equilibrium leads to a system of integro-differential equations in time domain. Viscous damping con be considered as a particular case with hereditary kernels reduced to the Dirac–delta functions.

In this paper, a new numerical method to find eigenenvalues and eigenvectors for linear symmetric nonproportional and nonviscous systems is proposed. We construct specially developed complex–valued functions, in particular as many as the number of modes. The recursion of these functions gives as a result iterative sequences which are able to converge (under certain conditions) up to the complex eigenvalues, also called fixed–points in this context. Together with the eigenvalues sequence, eigenvectors sequence is also derived.

A deep study on the convergence of the numerical method is carried out. For the analysis of any recursive scheme it is relevant to obtain the derivative of the recursive function at the fixed–points. In this work, a closed–form expression of the derivative of the recursive function is derived, showing up interesting relationships between the velocity of convergence, the nonproportionality of the system and the viscoelasticity (or nonviscousity). In general, it is proved that lightly damped systems present faster velocity of convergence, although under a linear rate. Some particular cases are analyzed by separate. Those related to light damping are of special interest since closed–forms expression have been derived depending only on a–priori information.

The proposed method is validated through three numerical examples. The two first examples are designed under the same geometry (6 degrees-of-freedom lumped–mass system), but with different damping models.

The first one presents a damper with a viscoelastic model based on exponential kernels whereas the second one has purely viscous dampers. In order to compare the effect of the damping level, two damping cases are discussed: high and light damping. The obtained convergence velocity of the recursive sequences results in great agreement with the theoretical results, both for nonviscous and viscous damping. The method is in general valid for the majority of the damping models used for engineering applications, although global convergence is not proved and special cases with highly damped systems could have repulsive fixed points. The third example shows how the proposed method behaves with continuous systems with different sizes. It is observed that the number of iterations remains constant as the size of the mesh increases. The theoretical derivations allow to predict this behaviour since the number iterations has been demonstrated to depend exclusively on the damping model but not on the number of structural degrees of freedom. Since the proposed recursive sequences are converging linearly, the velocity can be improved up to quadratic using the Aitken's accelerating method, specially useful for highly damped sproblems.

Acknowledgments

The author gratefully acknowledges the support and help provided by Professor Dr. Marcelo Epstein of the University of Calgary (Canada) in the edition of this manuscript during the Research Fellowship of the Author in Calgary during the spring and summer of 2017. The author also acknowledges the support of the Universitat Politècnica de València with its *Programa de Apoyo a la Carrera Académica del Profesorado 2017* oriented to Research Stays in other Universities and Research Centers.

References

[1] D. Golla, P. Hughes, Dynamics of viscoelastic structures - a time-domain, finite-element formulation, Journal of Applied Mechanics-Transactions of the ASME 52 (4) (1985) 897–906.

[2] S. Adhikari, Dynamics of non-viscously damped linear systems, Journal of Engineering Mechanics 128 (3) (2002) 328–339.

[3] N. Wagner, S. Adhikari, Symmetric state-space method for a class of nonviscously damped systems, AIAA Journal 41 (5) (2003) 951–956.

[4] M. Biot, Variational principles in irreversible thermodynamics with application to viscoelasticity, Physical Review 97 (6) (1955) 1463–1469.

[5] R. Bagley, P. Torvik, A theoretical basis for the application of fractional calculus to viscoelasticity, Journal of Rheology 27 (3) (1983) 201–210.

[6] R. Bagley, P. Torvik, Fractional calculus - a different approach to the analysis of viscoelastically damped structures, AIAA Journal 21 (5) (1983) 741–748.

[7] S. Adhikari, A reduced second-order approach for linear viscoelastic oscillators, Journal of Applied Mechanics-Transactions of the ASME 77 (4) (2010) 1–8.

[8] M. Lázaro, J. L. Pérez-Aparicio, M. Epstein, Computation of eigenvalues in proportionally damped viscoelastic structures based on the fixed-point iteration, Applied Mathematics and Computation 219 (8) (2012) 3511–3529.

[9] A. Muravyov, S. Hutton, Closed-form solutions and the eigenvalue problem for vibration of discrete viscoelastic systems, Journal of Applied Mechanics-Transactions of the ASME 64 (3) (1997) 684–691.

[10] A. Muravyov, Forced vibration responses of viscoelastic structure, Journal of Sound and Vibration 218 (5) (1998) 892–907.

[11] S. Menon, J. Tang, A state-space approach for the dynamic analysis of viscoelastic systems, Computers & Structures 82 (15-16) (2004) 1123 – 1130.

[12] A. Ruhe, Algorithms for nonlinear eigenvalue problem, SIAM Journal on Numerical Analysis 10 (4) (1973) 674–689.

[13] W. H. Yang, A method for eigenvalues of sparse λ-matrices, International Journal for Numerical Methods in Engineering 19 (6) (1983) 943–948.

[14] K. Singh, Y. Ram, Transcendental eigenvalue problem and its applications, AIAA Journal 40 (7) (2002) 1402–1407.

[15] K. V. Singh, Eigenvalue and eigenvector computation for discrete and continuous structures composed of viscoelastic materials, International Journal of Mechanical Sciences 110 (2016) 127 – 137.

[16] E. M. Daya, M. Potier-Ferry, A numerical method for nonlinear eigenvalue problems application to vibrations of viscoelastic structures, Computers & Structures 79 (5) (2001) 533 – 541.

[17] L. Duigou, E. M. Daya, M. Potier-Ferry, Iterative algorithms for non-linear eigenvalue problems. application to vibrations of viscoelastic shells, Computer Methods in Applied Mechanics and Engineering 192 (11-12) (2003) 1323 – 1335.

[18] S. Adhikari, B. Pascual, Eigenvalues of linear viscoelastic systems, Journal of Sound and Vibration 325 (4-5) (2009) 1000–1011.

[19] S. Adhikari, B. Pascual, Iterative methods for eigenvalues of viscoelastic systems, Journal of Vibration and Acoustics 133 (2) (2011) 021002.1–021002.7.

[20] F. Cortés, M. J. Elejabarrieta, Computational methods for complex eigenproblems in finite element analysis of structural systems with viscoelastic damping treatments, Computer Methods Appl. Mech. Engineering 195 (44-47) (2006) 6448–6462.
[21] F. Cortés, M. J. Elejabarrieta, An approximate numerical method for the complex eigenproblem in systems characterised by a structural damping matrix , Journal of Sound and Vibration 296 (1-2) (2006) 166–182.
[22] M. Martinez-Agirre, M. J. Elejabarrieta, Higher order eigensensitivities-based numerical method for the harmonic analysis of viscoelastically damped structures, International Journal for Numerical Methods in Engineering 88 (12) (2011) 1280–1296.
[23] M. Lázaro, Eigensolutions of non-proportionally damped systems based on continuous damping sensitivity, Journal of Sound and Vibration 363 (C) (2016) 532–544.
[24] M. Lázaro, Closed-form eigensolutions of nonviscously, nonproportionally damped systems based on continuous damping sensitivity, Journal of Sound and Vibration 413C (2018) 368–382.
[25] S. Adhikari, An iterative approach for nonproportionally damped systems, Mechanics Research Communications 38 (3) (2011) 226 – 230.
[26] M. Biot, Theory of stress-strain relations in anisotropic viscoelasticity and relaxation phenomena, Journal Of Applied Physics 25 (11) (1954) 1385–1391.
[27] P. Muller, Are the eigensolutions of a l-d.o.f. system with viscoelastic damping oscillatory or not?, Journal of Sound and Vibration 285 (1-2) (2005) 501–509.
[28] S. Adhikari, N. Wagner, Analysis of asymmetric nonviscously damped linear dynamic systems, Journal of Applied Mechanics (Transactions of ASME) 70 (6) (2003) 885–893.
[29] M. Lázaro, Nonviscous modes of nonproportionally damped viscoelastic systems, Journal of Applied Mechanics (Transactions of ASME) 82 (12) (2015) Art. 121011 (9 pp).
[30] T. Caughey, M. O'Kelly, Classical Normal Modes in Damped Linear Dynamic Systems, Journal of Applied Mechanics 32 (3) (1965) 583–588.
[31] S. Adhikari, Classical normal modes in non-viscously damped linear systems, AIAA Journal 39 (5) (2001) 978–980.
[32] S. Adhikari, Modal analysis of linear asymmetric non-conservative systems, ASCE Journal of Engineering Mechanics 125 (12) (1999) 1372–1379.
[33] A. M. Ostrowski, Solutions of Equations in Euclidean and Banach Spaces, Academic Press, 1973.
[34] T. Caughey, Classical normal modes in damped linear dynamic systems, Journal of Applied Mechanics 27 (1960) 269–271.
[35] S. Adhikari, Damping modelling using generalized proportional damping, Journal of Sound and Vibration 293 (2006) 156–170.
[36] J. Woodhouse, Linear damping models for structural vibration, Journal of Sound and Vibration 215 (3) (1998) 547–569.
[37] J. Woodhouse, Viscous damping identification in linear vibration, Journal of Sound and Vibration 203 (1998) 475–500.
[38] S. Papargyri-Beskou, D. Beskos, On critical viscous damping determination in linear discrete dynamic systems, ACTA MECHANICA 153 (1-2) (2002) 33–45.
[39] A. Aitken, On bernoulli's numerical solution of algebraic equations, Proceedings of the Royal Society of Edinburgh 46 (1926) 289–305.